Seasonal Variability of Groundwater Contribution to Watershed Discharge in Discontinuous Permafrost in the North Klondike River Valley, Yukon

Submitted by: Anthony Lapp

Thesis presented to the Faculty of Graduate and Postdoctoral Studies in partial fulfilment of the requirements for the degree of Master of Science in Earth Sciences

Department of Earth Sciences

Faculty of Science

University of Ottawa

Supervisor:

Dr. Ian D. Clark (Department of Earth Sciences)

Thesis Committee:

Denis Lacelle, University of Ottawa

Tim Patterson, Carleton University

Abstract

The objectives of this thesis were: (1) to quantify seasonal groundwater contribution to total stream discharge and (2) further our understanding of sub-arctic carbon sources and pathways within a sub-arctic discontinuous permafrost river catchment. Twenty-two samples were taken from the North Klondike River, 14 samples from 5 of its tributaries, and 46 rain and snowmelt samples from the Dawson City Airport, Yukon, Canada,. During the winter months, groundwater is responsible for greater than 95% of total river discharge. Spring freshet and summer flow bring snowmelt and precipitation, contributing anywhere from 30% to greater than 60% of total river discharge. Groundwater is characterised by high concentrations of geogenic solutes from weathering during recharge, dissolved inorganic carbon, and carbon-14 activities of 0.61 pMC. Tritium activities indicate a fast moving system, with groundwater ages measuring less than 10 years. The most significant discharge of organic carbon from the system is during spring freshet (434,192 kg carbon). Primary productivity within the system is estimated to be 10.2 grams of carbon per metre squared, with approximately 96% of carbon being sequestered or emitted as carbon dioxide.

Acknowledgements

I express my warm thanks to my supervisor Dr Ian Clark for his support, guidance, funding, and the opportunity to complete such a wonderful project. I would like to thank the staff in the G.G. Hatch Isotope Lab, Paul Middlestead, Wendy Albi, and Patricia Wickham, as well as Ping Zhang and Nimal DeSilva in Geochemistry Lab for their help with sample analysis. I should also thank Sarah Agosta, Carley Crann, Gilles St-Jean, and Normand St-Jean for their help with graphitization and carbon dating. I would like to thank my colleague Matt Herod for his guidance and support for all things Yukon and data analysis. A special thank you to Michael Grinter, Natalia Baranova, and Laurienne Bouchard for their help in the field, in collecting my samples, and keeping us alive up north. I would also like to thank Royce Freeman at the Tombstone Highway Maintenance Camp, for his help in collecting samples throughout 2014. I also thank Lynne Campo at Environment Canada for providing me with the North Klondike Discharge data. Thank you to Debra Blatter at the Dawson City Airport for collecting precipitation for the duration of my project. I give a special thanks to my good friend and colleague, Monika Wilk, for her help with tritium enrichment and all my lab work, as well as her constant support and guidance during my project.

I would like to thank my friends, for their help and encouragement over the past few years, and for lending their support when necessary. I am eternally grateful to my parents, and to my girlfriend Morgan McLellan, for their support, encouragement, and patience.

Table of Contents

List of Figures

List of Tables

1. Introduction

The hydrology of our arctic and subarctic watersheds is changing due to recent climate warming (Serreze *et al.* 2000; Walvoord and Striegl, 2007). Permafrost environments are hydrologically complex. Permafrost often controls water storage and drainage processes, by limiting water infiltration and interactions between near-surface and deeper sub-groundwaters. Hypothesized consequences of climate change include changes in groundwater recharge, pathways, and discharge to surface water. Groundwater behaviour in permafrost environments is an understudied topic, and has seen relatively little research over the past decade (Woo *et al.*, 2008; Carey and Pomeroy, 2009; Muskett and Romanovsky, 2009). There are several reasons for this lack of knowledge. Spatial coverage of hydrometric and climatic data networks in northern regions is sporadic, and with short, incomplete and discontinued data records. This, coupled with the arcane nature of groundwater makes carrying out hydrogeological research difficult in these environments. Initial research attempts to understand permafrost-related hydrogeology are often of short duration, lacking in measured hydrologic variables, and of limited spatial extent (Woo *et al.*, 2008). Although recent concerns about climate change have generated an increased interest in high-latitude hydrology (Zhao-ping *et al.*, 2010), there is still much about these systems that is poorly defined but necessary if we are to properly understand our northern watersheds.

This thesis is an attempt to further our understanding of groundwater hydrology in the sub-arctic. By definition, permafrost is ground that remains at or below $0^{o}C$ for at least two consecutive years (Woo, 2012). The North Klondike River, located in the Yukon's Tombstone Territorial Park, is an ideal site for the study of groundwater hydrology in a discontinuous permafrost zone, due to its proximity to Dawson City and the existing infrastructure within the watershed. The North Klondike River Valley lies right on the boundary between discontinuous and continuous permafrost and would be an ideal area to monitor climate induced permafrost changes. Logistically, the river is easily accessible along the Dempster highway and on foot. The Yukon government has maintained climatic and hydrologic monitoring stations for a period of approximately 40 years (1974 – 2015). The North Klondike River basin is very well defined, allowing for a full watershed level analysis. The Yukon government and local community were able to be engaged to help sample throughout the year, with the University

of Ottawa conducting high resolution sampling during major hydrologic events such as spring thaw.

Thawing permafrost has been hypothesized to allow deeper groundwater contribution to the drainage network and an increased active layer thickness resulting in deeper supra-permafrost pathways (Carey and Quinton, 2005; Petrone *et al.*, 2006; Frey and McClelland, 2009). As a result, stream flow geochemistry and the magnitude of runoff are expected to change. The hydrological response will transition from a rapid response to a slower more gradual response dominated by baseflow (Maclean *et al.*, 2014; Petrone et al., 2006; St. Jacques and Sauchyn, 2009). The hydrological transition to less permafrost has been hypothesized to show a decline in dissolved organic carbon (DOC) by rerouting subsurface flow through deeper mineral soils previously isolated by permafrost. Previous studies have examined carbon export from arctic and subarctic river basins (Walvoord and Striegl, 2007; Carey *et al.*, 2012; O'Donnell *et al.*, 2012), but they often focus on large rivers and watersheds which makes it difficult assess impacts of climate change.

One of the techniques to quantify and study total river discharge is the use of isotope hydrograph separation. This is a mass balance approach to separate individual hydrologic components including groundwater, surface runoff and precipitation (Clark and Fritz, 1997). Since the advent of isotope hydrograph separation, there has been an increase in hydrograph separation applications in new hydrologic areas, such as permafrost terrain. Historically, hydrograph separation has been limited to catchments located in humid temperate forest regions in southern Canada, central and Northern Europe, and parts of Australia, New Zealand and the USA (Buttle, 1994). The earliest example of work in permafrost terrain is that of Obradovic and Sklash (1986), but not until early 2000 did scientists begin to follow up on this work (Carey and Quinton, 2004; Hayashi *et al.*, 2004; St. Amour *et al.*, 2005; Boucher and Carey, 2010; Carey *et al.*, 2013). This study will build upon previous work done in permafrost environments and provide further insight into permafrost hydrology.

The majority of reporting on permafrost thaw and its impact on groundwater contributions to stream flow have been observed on large river systems in Canada and the United States such as the Yukon River and Porcupine River (Walvoord and Striegl, 2007), the Mackenzie and Peel River (St. Jacques and Sauchyn, 2009), and on large Russian rivers (Frey *et al.*, 2007;

Smith *et al.,* 2007). There has been less of an emphasis on understanding flow processes in headwater catchments, and how these are responding to climate change. Although there is strong evidence of climate change in northwestern North America, inter-annual variability of temperature and precipitation have complicated our understanding of the hydrological response to thawing permafrost. All of these components are crucial for creating an accurate hydrograph of the river and quantifying seasonal groundwater discharge.

There have been a number of studies assessing carbon export within arctic watersheds, but more is required if we are to gauge climate-based influences in these watersheds. Raymond *et al.* (2007) monitored dissolved organic carbon (DOC) quantity and ages within 5 of the largest arctic rivers (Yenisey, Lena, Ob', Mackenzie, Yukon), with regular sampling throughout 2004-2005, between the months of March and October. The authors concluded that these arctic rivers export ~2.5x more organic carbon than temperate rivers of similar watershed sizes and water discharge. Spencer *et al.* (2008) measured DOC quantity and composition from large Yukon Rivers within the Yukon River basin from 2001-2005, however sampling was performed infrequently. This was an attempt to differentiate and source the organic carbon being exported within arctic watersheds. Aiken *et al.* (2014) heavily sampled the Yukon River and 15 tributaries of the Yukon River, as well as glacial meltwater, groundwater, and soilwater to assess the quantity and age of dissolved organic carbon within the watershed, and how it might react to climate effects. However, the ability to observe and quantify changes in DOC within the watershed is made more complicated by the diversity of sub-watersheds within the Yukon River basin. A more effective strategy to assess climate-based influences in arctic river basins would be the identification and monitoring of smaller tributaries sensitive to glacial melting, permafrost thaw, and changes in watershed hydrology.

Granger Creek, located within the Wolf Creek Research Basin (South Yukon), has been extensively studied for this reason (Carey, 2003; Carey and Quinton, 2004; Carey and Quinton 2005; Petrone *et al.,* 2006*;* Walvoord and Streigl, 2007; Boucher and Carey, 2010). Granger Creek is located within the discontinuous permafrost zone, and has been the subject of hydrological research since 1992. The North Klondike River is an ideal candidate to emulate the type of research that has been undertaken within the Wolf Creek Research Basin. The North Klondike River is located within the discontinuous-continuous permafrost boundary,

and would be useful for monitoring permafrost thaw, carbon export, and any changes in hydrology.

The primary objectives of this thesis will be (1) to quantify seasonal groundwater contribution to total stream discharge and (2) further our understanding of sub-arctic carbon sources and pathways. This will be achieved by sampling throughout the year, through the seasons and during all major hydraulic events such as baseflow and spring freshet. River water samples were taken for geochemical analysis, stable isotope analysis, dissolved inorganic and organic carbon, tritium, and radiocarbon. Infrastructure exists in the area that allowed samples to be taken during the winter, where previous studies have often neglected to sample. Stable isotope hydrograph-separation techniques will be used to assess the relative contribution of groundwater to total river discharge.

1.1 Hydrologic Cycle

The hydrologic cycle is a complex web of water movement between the major reservoirs driven by solar energy. Of the water on earth, 96.5% is in the oceans. Of the fresh water, 69% is in the solid form in glaciers, 1% is liquid surface water bodies, and the remaining 30% exists as groundwater. There are three major components of the global water cycle: (1) the oceans lose more water by evaporation than they gain by precipitation; (2) land surfaces received more water by precipitation than they lose by evaporation or transpiration; (3) the excess water on land returns to the oceans as runoff, thereby balancing the deficit in the ocean-atmosphere exchange (Dingman, 2008).

Rivers are the major routes by which excess water on the continents returns to the oceans. The rate of direct groundwater input to the oceans is not well established, but is thought to be small compared to river flows. From the point of view of the global hydrologic cycle, lakes can be simply thought as wide places in rivers acting as temporary reservoirs.

Groundwater is the water located beneath the earth's surface in soil pore spaces and in the fractures of rock formations. Most water enters the groundwater reservoir by infiltrating downwards and arriving at the water table as recharge. The water table is the upper boundary of the groundwater-zone, where the water pressure is equal to atmospheric pressure and can fluctuate according to atmospheric pressure changes. The material at and below the water table will be completely saturated with water.

A unit of rock or material that is saturated with water, and from which water could be extracted using a well, is called an aquifer. An aquitard can be considered the opposite of an aquifer, and is a unit of material that would restrict the flow of groundwater, typically from one aquifer to another. Aquifers which are open to the atmosphere are classified as unconfined aquifers, with their upper boundary being the water table. Most often the shallowest aquifer at a given location is unconfined. If an aquifer is saturated throughout and bounded above and below by aquitard formations, it would be a confined aquifer.

Under normal conditions, groundwater will discharge into rivers, lakes, coastal areas, or directly into the ocean. Groundwater can also migrate upwards into the capillary fringe,

leaving the groundwater reservoir (Dingman, 2008). The rate at which water moves within a porous medium depends upon its hydraulic conductivity and total potential energy.

Hydraulic conductivity is a measure of the rate at which water can pass through a porous medium. The rate of flow depends on the size of pores and dilation of cracks, the density and dimensions of fissures in rocks, connectivity of flow pathways, and the viscosity of the fluid. Temperatures below freezing, such as in permafrost areas, can drastically reduce the hydraulic conductivity as unfrozen water content decreases and the pores and cracks within the medium are increasingly filled with ice (Woo, 2012).

Evapotranspiration (ET) plays an important role in governing the soil moisture, vegetation productivity, carbon cycling, and water budget in terrestrial ecosystems(Yuan *et al*., 2010). On average, nearly two thirds of precipitation that falls over global land is returned to the atmosphere via ET. However ET is one of the most difficult components of the water cycle to estimate due to the large number of controlling factors including climate, plant biophysics, soil properties, and topography (Dirmeyer *et al.*, 2006). Over the long term, the difference between precipitation and ET is the water available for direct human use and management. Accurate quantitative assessments of water resources and the effects of climate and land use change on those resources require a quantitative understanding of ET.

Transpiration is the evaporation of water from the vascular system of plants into the atmosphere. The process involves absorption of soil water by plant roots; translocation through the vascular system of the roots, stem and branches to the leaves; and translocation through the vascular system of the leaf to the walls of stomatal cavities where evaporation takes place. The water vapour in these cavities moves into the ambient air through the openings in the leaf surface called stomata (Dingman, 2008). It is important to note that transpiration is a physical, and not a metabolic process. Water in the transpiration stream is pulled through the plant by potential-energy gradients, driven by the movement of water vapour into the air through the stomata in response to a vapor-pressure difference.

Since transpiration and evaporation are both physical process, the most common method of estimating actual ET from a land area is in the application of the water-balance equation in the form:

$$ET = W - Q - G_{out}$$

where W is precipitation, Q is streamflow, and G_{out} is groundwater outflow. Once transpiration has been calculated, primary productivity can be estimated with published carbon use efficiencies.

1.2 Hydrology in Permafrost Regions

Permafrost is a condition in which soils and/or their underlying parent materials remain frozen ($T < 0^oC$) throughout the year (Woo, 2012). There can be a thin surface layer that thaws in the summer and is referred to as the active layer, however there are contrasting definitions of the concept (Burn, 1998). Muller (1974) defines the lower boundary of the active layer as the top of permafrost, which is the maximum seasonal penetration of temperatures above 0°C. Van Everdingen (1976) differentiated between the thermal status of the ground even further, as well as the phase of water in the ground. Van Everdingen suggested the term 'cryotic' to describe ground below 0°C, and reserved 'frozen' for materials containing ice. By this definition, the active layer is a hydrologic, not thermal, boundary and is defined by the depth of the freezing-point depression, which requires extensive laboratory testing of soils to determine rendering this variable unsuitable for field use. For the vast majority of terrestrial environments, this freezing-point depression for ice nucleation is less than 0.2 °C, and for practical purposes both definitions are in agreement.

Permafrost is believed to act as an aquitard, and can strongly restrict and influence subsurface flow. The influence of permafrost on hydrology depends upon its continuity within the ground. In continuous permafrost environments, deep drainage is largely restricted and subsurface aquifers are isolated from the surface. Compared to areas of discontinuous permafrost, where coverage is interrupted allowing deeper subsurface aquifers to more easily interact with surface waters. Permafrost hydrology is considered cold region hydrology, and concerned with the direct or indirect effects of perennially frozen ground (Woo, 2012).

Figure 1 is a conceptualisation of the water cycle in a permafrost environment. Precipitation arrives mostly in the forms of snow in winter and rain in summer. Snowfall accumulates seasonally over winter and in spring and summer, rainfall and snow meltwater will easily saturate any thawed soil. Any water that cannot enter the ground will become surface runoff to feed rivers, wetlands and lakes. Sometimes water is able to infiltrate deeper into the ground and recharge groundwater reservoirs that can lie above, within or below the permafrost. Groundwater discharge can occur in summer and winter. During winter it can freeze above ground or within the active layer or emerge as springs that feed streams, wetlands, or lakes.

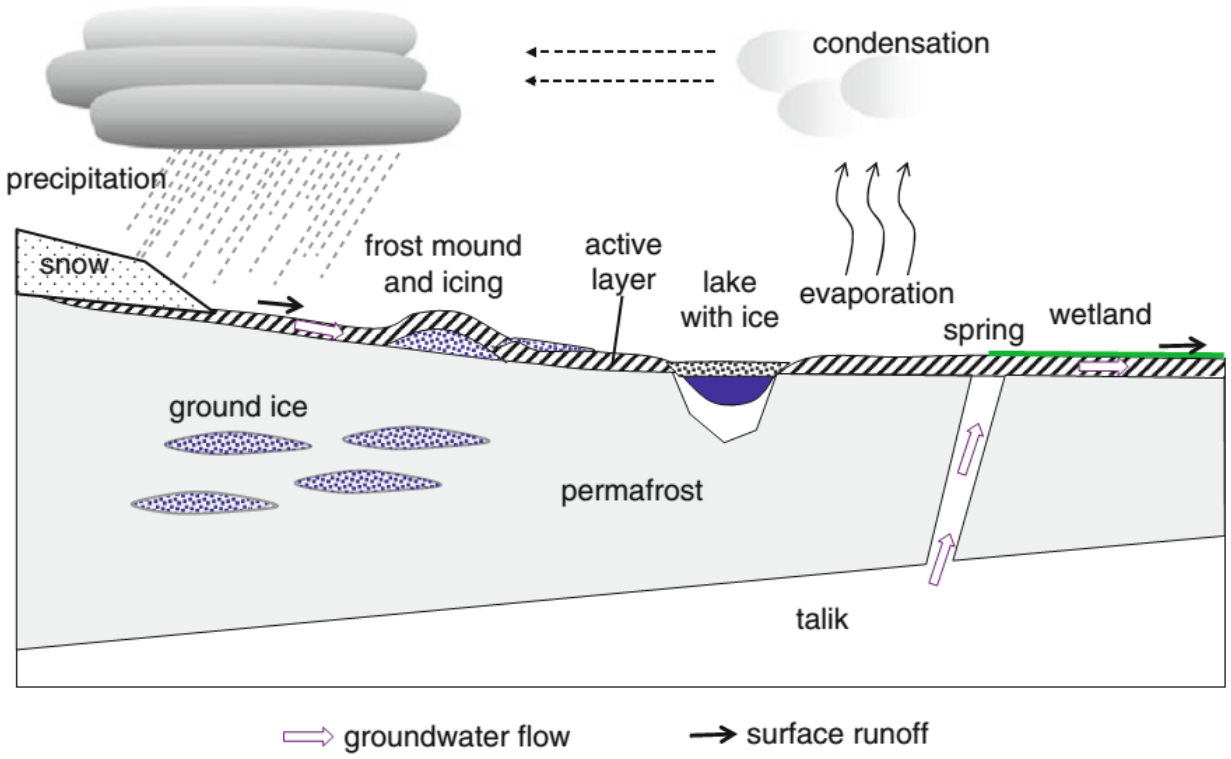

Figure 1 Conceptual model of permafrost hydrology showing the circulation and storage of water (Woo, 2012).

Permafrost does not necessarily need to contain water or ice. It can also become saturated with unfrozen water if ice formation is prevented. The freezing point of water can be depressed by the adsorption of water onto soil particles, the presence of dissolved minerals, and increased pressure (Woo, 2012). Most often, unfrozen water and ice co-exist in permafrost resulting in blockage and the restriction of flow within the frozen ground. Permafrost is often considered to behave as an aquiclude or acquitard. As such, most groundwater is often found in the thawed zones surrounding permafrost. Groundwater movement can occur above, within and beneath the permafrost, and is referred to as suprapermafrost, intrapermafrost and subpermafrost groundwater. Figure 2 is a conceptual model of these different classifications of groundwater in permafrost terrain. Permafrost environments also contain areas of talik, year-round unfrozen ground, providing passage for deeper subsurface aquifers to connect with water above the permafrost table. Heated groundwater or mineralized water can create hydrothermal or hydrochemical pathways. Talik may also form due to the proximity of a surface water body, or due to the presence of faults and permeable geologic units (Woo, 2012).

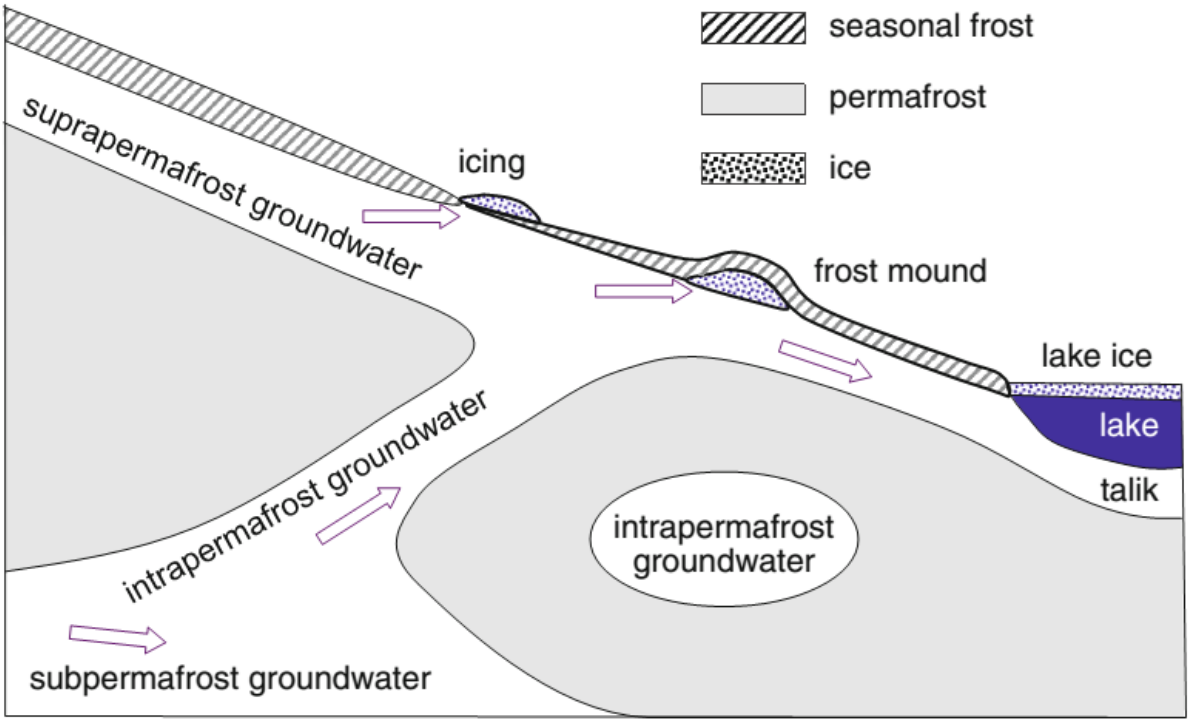

Figure 2 Conceptual model of permafrost groundwater sources and their pathways, showing supra-permafrost (above permafrost), intra-permafrost (within permafrost) and sub-permafrost (below permafrost) groundwater (Woo, 2012).

1.3 Carbon Cycle

There are two major carbon-based components in any hydrological system: inorganic carbon and organic carbon. They can be measured as either total carbon or dissolved carbon, an operational classification defined as compounds below 0.45 µm. In the North Klondike River valley major carbon reservoirs are the atmosphere, the terrestrial biosphere, and sediments/minerals and non-living organic matter. Inorganic carbon, measured as dissolved inorganic carbon (DIC), is gained by the dissolution of atmospheric CO_2 in fresh groundwater, and the weathering of carbonate or silicate materials. Organic carbon is a product of plant photosynthesis and microbial activity which sequesters atmospheric CO_2 into organic compounds. These organic compounds can then be broken down and released into the catchment as dissolved organic carbon (DOC). The most common soil-derived organic matter are humic acid substances, with high molecular weights. Low molecular weight organic matter makes up the remainder which includes cellulose, protein, and other organic acids such as carboxylic, acetic, and amino acids (Clark and Fritz 1997). In Arctic regions and boreal regions of the Northern Hemisphere where permafrost is present, the decomposition of DOC and release of both DIC and DOC is restricted to the point that large carbon reservoirs develop.

Organic carbon stored in permafrost is composed of carbon frozen at depth in peatlands (20% to 60% carbon) and carbon intermixed with mineral soils (<1% to 20% carbon), depending on the physiographic characteristics of the region (Schurr *et al.,* 2008). Organic carbon is introduced to the active layer and near-surface permafrost through plant photosynthesis and growth. Organic material, and subsequently the active layer, accumulate and grow over the years due to impeded microbial decomposition (Rivkina, *et al.,* 2000) and sediment and silt deposition. As organic and mineral soil accumulates, organic carbon at the bottom of the active layer becomes incorporated into the rising permafrost. Alternatively, organic carbon may be mixed into different soils layers due to repeated freeze thaw cycles, a process known as cryoturbation. As a result of these two mechanisms, it is not uncommon for organic carbon pools to be at much greater depth (Schirreister *et al.*, 2002; Zimon *et al.*, 2006).

Arctic and sub-Arctic river basins yield a large amount of water and terrigeneous dissolved organic carbon to the oceans (Raymond *et al.* 2007). The export of DOC is strongly seasonally dependent (Aiken *et al.* 2014), with a maximum organic carbon concentration in conjunction

with the period of maximum discharge during the spring freshet. Radiocarbon age and composition is also seasonally dependent, with the oldest DOC transport occurring under ice during winter months, and the youngest DOC during the spring freshet when discharge is greatest (Aiken *et al.,* 2014).

Under a warming climate, release of carbon from permafrost back to the atmosphere will occur primarily through accelerated microbial decomposition (Hartley *et al.,* 2008; Conant *et al.,* 2011). As high-latitude ecosystems cross the freezing-point threshold, there are a number of other ecosystem factors such as energy balance and element cycling that are linked to permafrost thawing. These other changes could further accelerate carbon release, while others can help offset carbon released from thawing permafrost. Higher temperatures can stimulate photosynthesis and lengthen growing seasons. This can increase carbon storage in plant biomass and subsequently in new soil organic matter (Myneni*et al.,* 1997). These higher temperatures and increased microbial activity can also increase nutrient availability, which often has a greater effect on plant growth than temperature (Chapin and Shaver, 1996). Plant species composition can also change, as the availability of carbon increases, i.e. low C:N soil organic matter becomes replaced with higher C:N plant biomass (Shaver *et al.* 2000).

The energy balance of northern ecosystems can potentially change as a result of these changes in Arctic carbon cycling. Increasing temperatures can be expected to move the boreal treeline northward and alter plant species composition (increase in shrub cover). This has the potential to increase solar radiation absorption, leading to local warming in the summertime (Schurr*et al.,* 2008). Alternatively, warmer climates bring about an increase in fire frequency (Flannigan *et al.,* 2005), capable of altering boreal forests proportions of broadleaf deciduous trees. These early-successional species can reflect more solar radiation compared to the needle-leaved evergreens, creating a cooling effect during the summer. Despite the effects of thawing permafrost that can increase the carbon storage of arctic ecosystems and alter energy balances, scientists still predict a greater loss of carbon then what can be sequestered by these changes (Schurr*et al.,* 2008).

1.4 Stable and Radio-isotopes

Stable- and radio-isotopes are a common tool used in hydrological research for their ability to provide a greater insight into physical and chemical processes. Stable isotopes of interest include oxygen-18 (^{18}O) and deuterium (^{2}H), which are incorporated within water molecules and exhibit systematic spatial and temporal variations as they fractionate within the water-cycle. This fractionation produces a natural label for the water and can be then used to study hydrological and climatic processes (Clark and Fritz, 1997; Gibson *et al.,* 2005). Water isotopes are reported relative to the SMOW (Standard Mean Ocean Water) standard or the modern equivalent VSMOW (Vienna-SMOW) standard. The average relationship between hydrogen and oxygen isotope ratios in natural terrestrial waters can be expressed as a worldwide average, and when plotted on a graph, creates a global meteoric water line (GMWL) displaying a linear correlation. A meteoric water line can be calculated for a given area, based on precipitation that falls within that area. This local meteoric water line (LMWL) can be used as a baseline for all water within a catchment. Water that deviates from this linear correlation are a result of kinetic fractionations, such as evaporation or freezing (Clark and Fritz, 1997).

Provided there are no phase changes, additional inputs, or fractionation along the flow path, ^{18}O and ^{2}H act as conservative groundwater tracers. Groundwater stable isotope values are typically a reflection of prevailing atmospheric conditions. With knowledge of precipitation isotope values, and ground water isotope values, it is even possible to infer the elevation of precipitation that recharged the aquifer (Blasch and Bryson, 2007). At higher altitudes, where the average temperatures are lower, precipitation will be isotopically depleted (Clark and Fritz, 1997). Using this knowledge, one can distinguish between groundwater recharged at high vs low altitudes.

Carbon-13 is another stable isotope of interest, and is an excellent tracer of carbonate evolution in groundwaters because of the large variations in carbon reserves. Carbon isotope ratios are often reported relative to the PDB (Pee Dee Belemnite) or equivalent VPDB (Vienna PDB) standard. Atmospheric carbon, with a $\delta^{13}C \sim -7‰$ and decreasing due to fossil fuel combustion, is sequestered into the soil through photosynthesis and the production of organic matter (in the form of carbohydrates). There are three principal photosynthetic cycles, the Calvin or C_3cycle, the Hatch-Slack or C_4cycle, and the Crassulacean acid metabolism (CAM) cycle (Clark and

Fritz, 1997). C_3 pathways operates in about ~85% if plant species, C_4 pathways within less than ~5%, and CAM pathways operate in the remaining ~10%.

C_3 plants dominate the North Klondike River valley (Kojima, 1996), and are responsible for carbon fixation within the soil. The overall process of converting CO_2 into carbohydrates results in a net depletion of 22‰ from C_3photosynthesis, with soil carbon ranging between -24‰ and -30‰. C_4 photosynthesis will create a soil carbon range between -10‰ and -16‰. As organic material accumulates, microbial activity will begin to convert organic material back into CO_2, which will have the same $\delta^{13}C$ as the vegetation.

Groundwater DIC and $\delta^{13}C_{DIC}$ are directly related to weathering within the soil and within the aquifer. The interaction of ground water and marine carbonates has been studied extensively. Marine carbonates have similar $\delta^{13}C$ to that of the reference VPDB ($\delta^{13}C \sim 0‰$). As carbonate dissolves by interactions with groundwater, the $\delta^{13}C_{DIC}$ will change to more enriched values. Open systems have a continual supply of CO_2 supplied by the soil, so the $\delta^{13}C_{DIC}$of the groundwater will be controlled by the $\delta^{13}C$entering the system vs the dissolution of carbonate ($\delta^{13}C \sim 0‰$). Groundwater in open systems will retain a P_{CO2} close to that of the soil, with a slightly enriched $\delta^{13}C$, and a high DIC concentration. In a closed system, the $\delta^{13}C$will be diluted by DIC from carbonate dissolution ($\delta^{13}C \sim 0‰$). These systems are characterized by a lower P_{CO2}, a more enriched $\delta^{13}C$ and a lower DIC concentration. Since the $\delta^{13}C$ becomes enriched in both systems, the use of $\delta^{13}C$ alone becomes less effective. Carbon-14 measurements can be useful to evaluate how open a system is, as DIC derived from the soil has a modern ^{14}C signal, whereas DIC from calcite dissolution has no ^{14}C activity (Clark and Fritz, 1997).

A radio-isotope of interest is the nuclide tritium (^3H), which can be incorporated within water molecules and is the only isotope that can actually date young groundwater directly, whereas indirect dating can be accomplished using radium-226 or radon-222. Tritium can be naturally produced by cosmic radiation, and combines with stratospheric oxygen to form water.

$$^{14}_{7}N + {}^{1}_{o}n \rightarrow {}^{12}_{6}C + {}^{3}_{1}H$$

$$^{3}H + O_2 \rightarrow {}^{3}HO_2 \rightarrow {}^{1}H\,{}^{3}HO$$

Tritium undergoes weak beta decay into helium-3, with a half-life of 12.3 years.

$$^{3}\mathrm{H} \rightarrow \ ^{3}\mathrm{He} + \beta^{-}$$

Tritium can also be anthropogenic in origin. The more abundant source of tritium was produced from the testing of thermonuclear bombs between 1951 and 1980. This anthropogenic source has been mostly washed from the atmosphere, and global precipitation levels of tritium have almost returned to pre-1950s levels (Figure 3). Thermonuclear tritium can still be found in slowly moving ground waters, but in more recent waters the natural ^{3}H is now relied upon (Clark and Fritz, 1997). This tritium can be amplified through electrolytic enrichment allowing for a more accurate analysis.

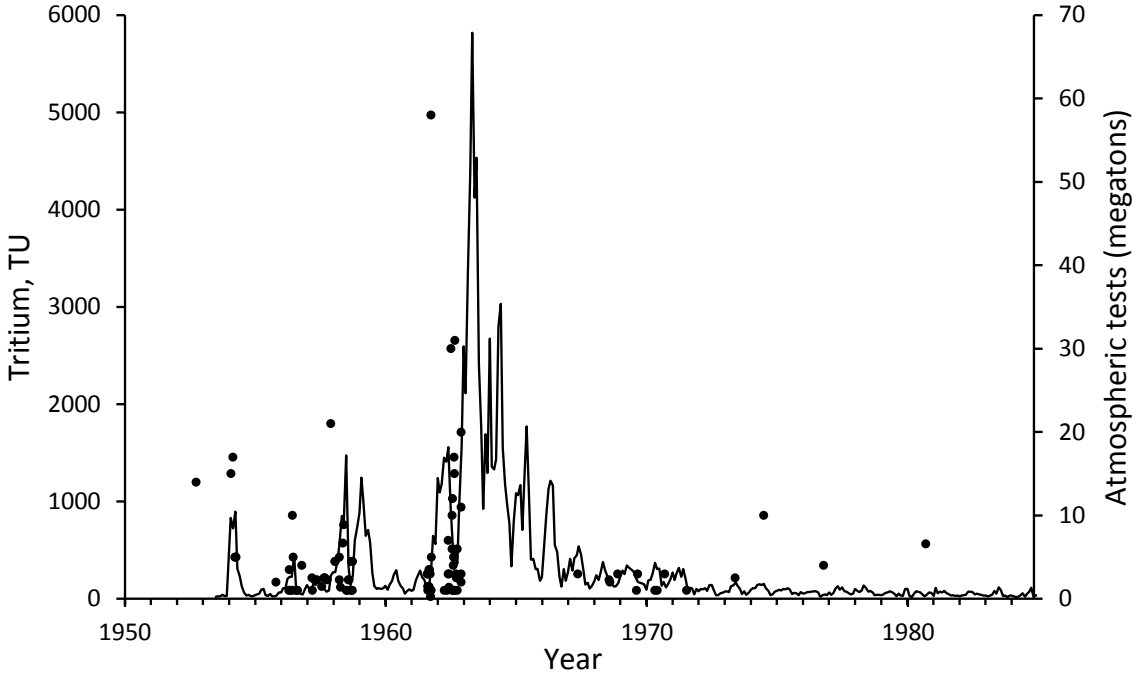

Figure 3 Tritium activity (TU) in precipitation and nuclear bomb tests from the 1950s to the 1990s (Clark, 2015).

Carbon-14 is another radio-isotope commonly used in estimating the age of paleo- and fossil groundwaters. This method is based upon the incorporation of atmospherically derived ^{14}C into photosynthesis. With a half-life of 5730 years, it can be effectively used to date groundwater accurately to about 30,000 years. The effectiveness of dating is a function of preservation, contamination, and analytical precision, not necessarily the half-life.

^{14}C is produced in the upper layers of the troposphere and the stratosphere by thermal neutrons absorbed by nitrogen atoms (Clark and Fritz, 1997; Geyh, 2000).

$$^{1}n + {}^{14}N \rightarrow {}^{14}C + {}^{1}p$$

This ^{14}C then oxidizes to carbon dioxide where it either dissolves into ocean waters or is consumed by vegetation during photosynthesis. This radiocarbon is then sequestered into the soil by the production of organic material and root respiration. Bacterial degradation of this organic material coupled with plant respiration sequesters a large amount of CO_2 into soils. The atmosphere contains about 400 ppmv (P_{CO2}~ $10^{-3.4}$), while soils can contain between 3000 to 30,000 ppmv (P_{CO2}~ $10^{-2.5}$ to $10^{-1.5}$). The result is a large reservoir of ^{14}C into the soil zone and serves as the pathway of ^{14}C into groundwater via recharge through the soil. ^{14}C activities are commonly reported as either a ratio of ^{14}C/^{12}C, with a higher ratio representing a greater portion of modern carbon, or in years before 1950. This practise of reporting relative to 1950 is to allow an easier comparison between published radiocarbon dates.

If all the ^{14}C washed from the soils remains with the groundwater along its flow path, without any dilution or loss, its decay can be used as a measure of age. However, the practical truth is that some ^{14}C is lost to dilution and to geochemical processes both within the soil and the aquifer itself,such as carbonate dissolution.

2. Introduction to the North Klondike River Valley

The North Klondike River (N 64°00’07.1”, W 138°35’45.0”) is situated in Central Yukon, approximately 68 km north east of Dawson City (Figure 4). The North Klondike has its source in the Southern Ogilvie Mountains., within Tombstone Territorial Park. The North Klondike River is a tributary of the Yukon River and a part of the Yukon River watershed. Approximate latitudes of the North Klondike River valley range from 64º00’ to 64º30’N and approximate longitudes from 138º00’ to 138º45’W, with an elevation range from 600 to 1000m above sea level (Kojima, 1997). Figure 5 shows the North Klondike River watershed including locations of sampled tributaries, meteorological station, as well as the discharge monitoring station where North Klondike River water samples were taken.

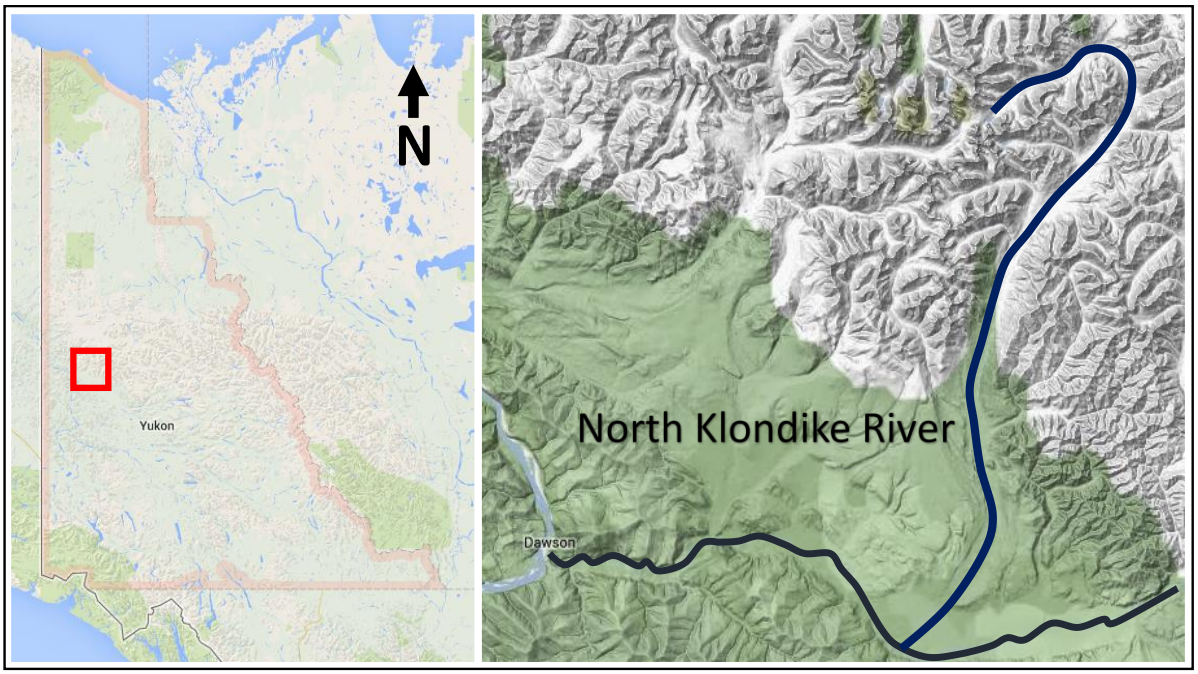

Figure 4 Location of the study site within the Yukon, Canada. The red star indicates the beginning of the North Klondike River in the Tombstone Mountain Range. The dark blue line represents the North Klondike River, and the lighter blue line represents the Klondike River (Google Maps, 2013).

The North Klondike River resides in the Mackenzie Mountain ecoregion and can be thought of as separating northern Yukon from Central Yukon. The entire ecoregion lies within the Cordilleran Foreland Fold and Thrust Belt, with the rock units and structures largely defining the landscape (Ecoregions of the Yukon Territory, pg 141, 2004). Since 1961, the Geological survey of Canada has mapped the geology of the entire region (Figure 6). Valley bottoms and the lower portion of the catchment are unconsolidated glacial and alluvial deposits (unit 26)

left behind from localized valley glaciation. These deposits dominate valley bottoms and the lower portion of the catchment. There are two distinct mountain ranges within the catchment, Antimony Mountain on the south and east side of the river and Tombstone Mountain on the west and north.

The Antimony Mountains consist of exposed Cambrian bedrock (unit 3), and the Road River Formation (unit 9), crystalline rocks containing small amounts of limestone. The Tombstone Mountains are composed of 4 different cretaceous units (18-21), showing an igneous intrusion, surrounded by altered rock units. Above the Tombstone Mountains is the Lower Schist (unit 17) which contains a few tributaries and represents the northern extent of the North Klondike River catchment. Although some of the units contain trace amounts of limestone and other sedimentary rocks, there are no significant sedimentary formations. Extensive faulting can be seen within the Tombstone Mountain range but not within the Antimony Mountain range.

The North Klondike River contains an area of aufeis, a sheet-like mass of layered ice formed by the successive flows of groundwater (Xu and Pollard, 1997). This aufeis is located upstream of Black Shale Creek, and is an indicator of a strong groundwater presence all year round, within this watershed. Apart from the North Klondike River itself, 5 separate tributaries were sampled within the watershed. Black shale creek, aptly named for the surrounding geology, drains within a geological unit containing shales, slates, and phyllites. Vegetation at this elevation changes to open woodlands. The other tributaries, Cairnes Creek, Grizzly Creek, Scout Car Creek, and Bensen Creek were chosen due to their size, location within the watershed, and easy access for sampling.

Kojima (1997) was the first to study flora within the valley. The North Klondike River valley belongs to the boreal forest region, characterised by coniferous forests interspersed with wetlands and bogs. Soils are rich in organic material and are underlain with permafrost at a depth of approximately 30-40cm. Gentle lower slopes of the valley are entirely covered by closed forests consisting of white spruce and the occasional black spruce. Above the forest line, 1000m above sea level on south slopes and 800m on north slopes, close forest changes to open woodland, followed by extensive shrub tundra and dwarf birch (Kojima, 1997).

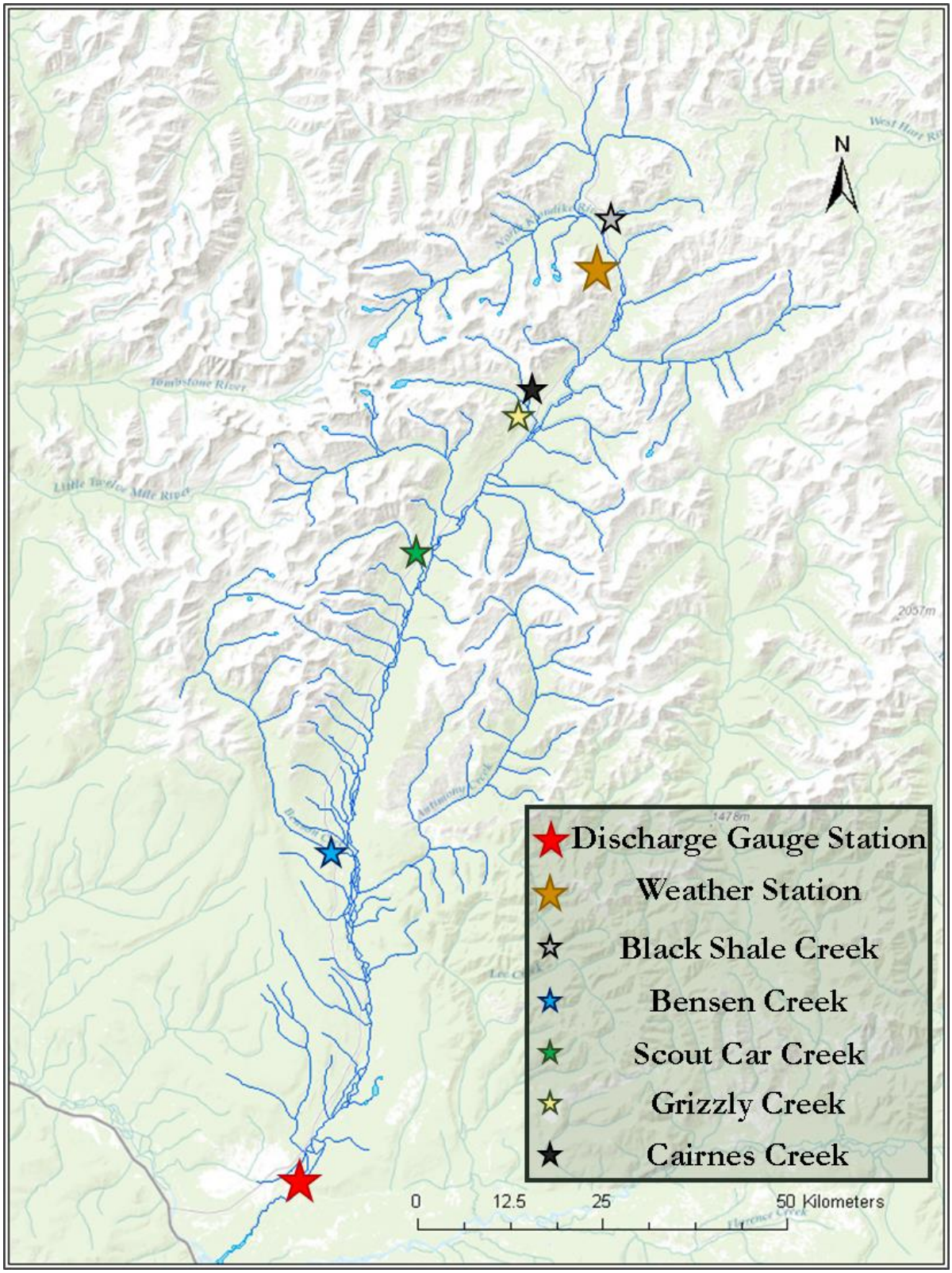

Figure 5 The North Klondike River situated within the North Klondike River valley. Sampled tributaries are shown, as well as the weather station within the park, and the discharge monitoring station where North Klondike River samples were taken.

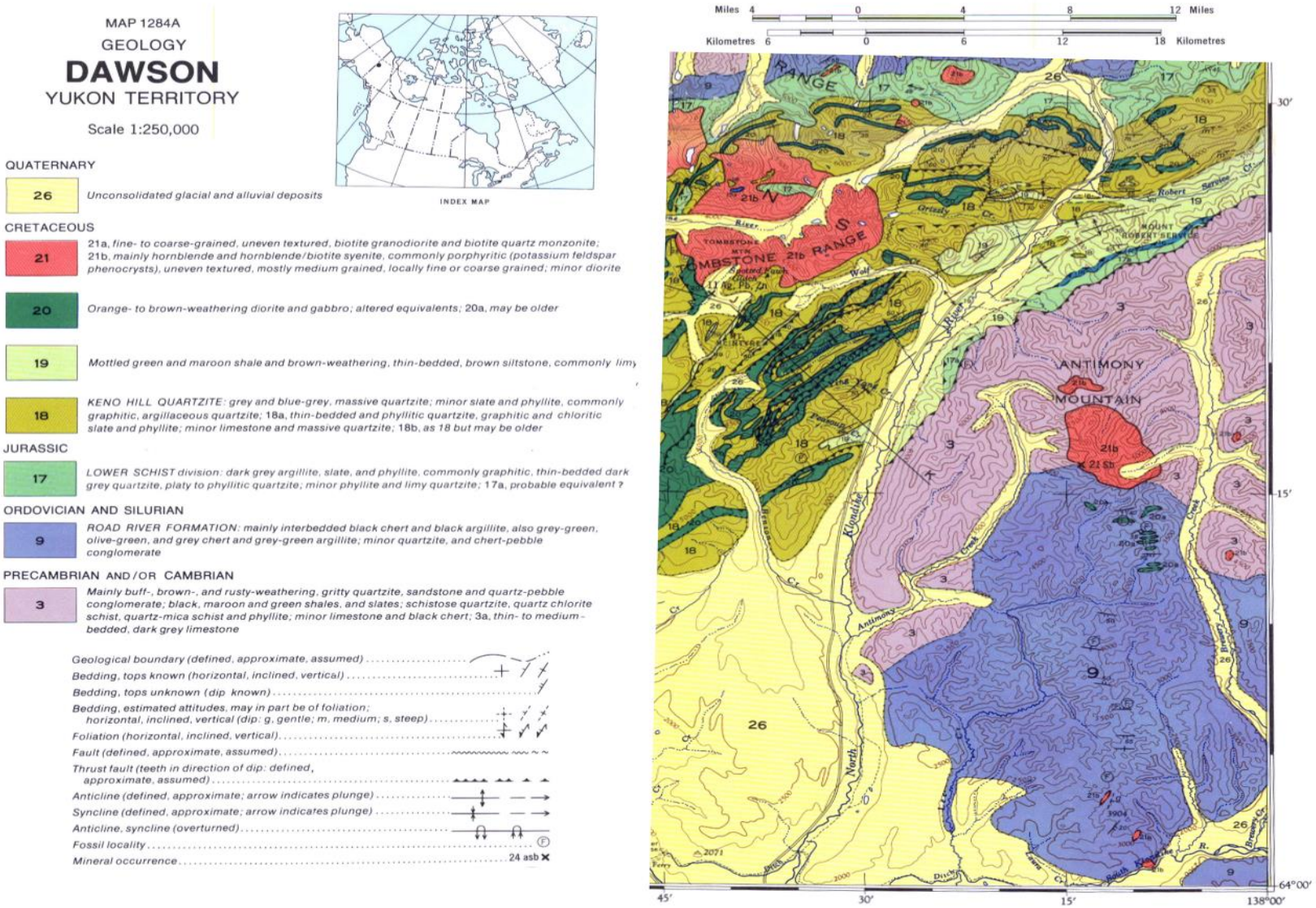

Figure 6 Excerpt from the Geological Map 1284A Dawson, Yukon Territory, showing Tombstone Territorial Park (Geological Survey Canada, 1972).

2.1 Permafrost in the North Klondike River Valley

Although this ecoregion straddles the southern boundary of the continuous permafrost zone, permafrost is found almost entirely throughout this region due to the elevation, with near surface temperatures above -4^{o}C. Permafrost is discontinuous but found to be very extensive within the valley and on north-facing slopes where peat can accumulate and provide insulation. Permafrost is found at a depth of approximately 40 cm in the valley bottom (Kojima, 1996). Figure 7 is an excerpt from one of the few maps available that include permafrost and ground ice conditions within the North Klondike River Valley (Geological Survey Canada, 1987). Green and yellow sections are classified as intermediate discontinuous permafrost, where permafrost underlies about half (~50%) the exposed land surface area. Valley slopes, north facing-slopes, and high elevations are classified as extensive discontinuous permafrost, where permafrost underlies more than half (50-90%) of the exposed land surface area. These areas are further denoted according to their ground ice content. Ice content is low to moderate in valley bottoms (3LM), with material frozen as thin seams, lenses, and wedges. Permafrost is found at a much greater distribution above the valley bottom, with low (3LM) to medium (4LM) ice content found on mountain slopes. The most elevated areas of this region, show little (4NL) to no ice content (4N) as the ground cover is primarily cobbles, boulders, and exposed rock units (Geological Survey Canada, 1987).

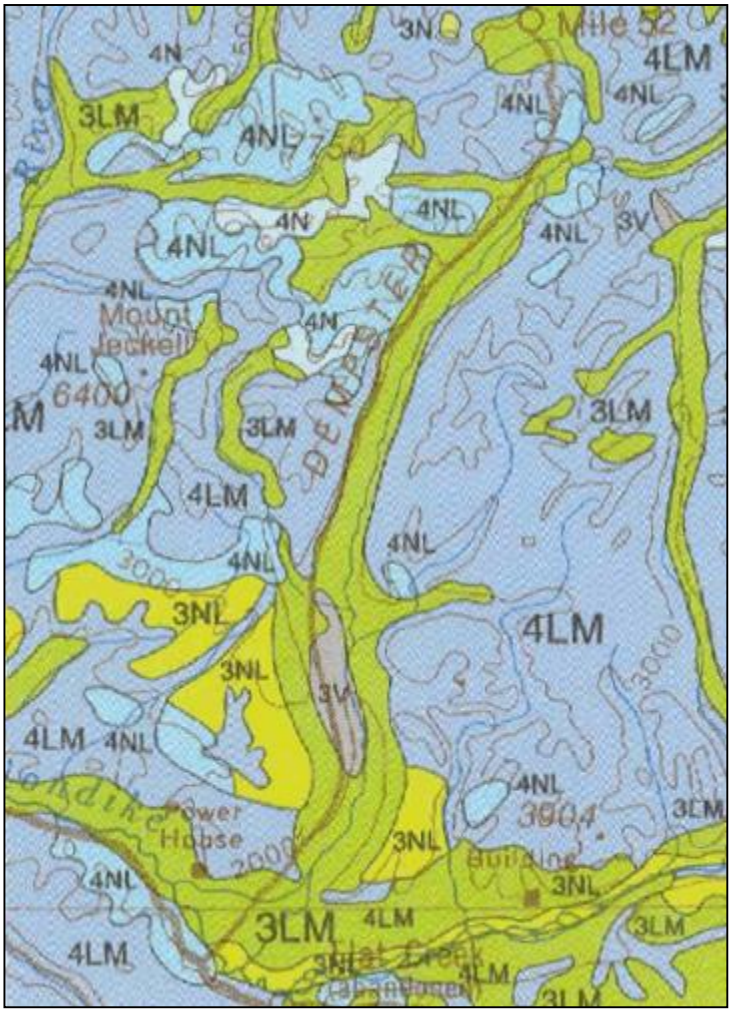

Figure 7 Ground Ice and Permafrost in the North Klondike River valley (Geological Survey of Canada, 1987). The North Klondike River can be seen following the Dempster Highway Northwards.

3. Methods

3.1 Sample Collection

Field work was conducted between August 2013 and August 2014. Preliminary sampling was conducted on August 1st to August 25th, 2013, to determine which tributaries would be sampled as well as contacting and enlisting local personal for sample collection. Water samples were taken from the North Klondike River by the Yukon Government Highway Tombstone maintenance camp from January 7th to August 19th, 2014, approximately every 2 weeks from the same location. River water was taken in clean, sterile, 1-liter Nalgene bottles and tape sealed. Once these samples were returned to the University of Ottawa, water was filtered using 0.45µm nitrile filters and aliquoted into 10ml falcon tubes for geochemical analysis, and 40ml EPA vials for DOC/DIC and $\delta^{13}C$ analysis. Water required for radiocarbon was filtered using 0.45µm nitrile filters and injected into a clean, sterile, baked, and evacuated 1L glass bottles prior to CO_2 extraction.

Personal at the Dawson City Airport collected precipitation from August 1st 2013 to August 23rd 2014, in order to establish a LMWL. Precipitation was collected from the meteorological monitoring station and stored in clean and sterile 50ml falcon tubes or 125ml Nalgene bottles. The University of Ottawa returned on April 14th to 25th 2014 to sample under ice and the onset of spring freshet, with a return trip from May 8th to 22nd to sample during spring freshet. Climate data was provided by the Government of Canada and Environment Yukon. Environment Canada provided the daily mean discharge data for the North Klondike River from 1974-2014. Yukon Parks also provided climate data for 2014 from within the North Klondike River basin at the Tombstone Interpretative Center.

3.2 Laboratory Analysis

Precipitation and river water samples were shipped back to the University of Ottawa for analysis. All water samples were analyzed for major ion concentrations, $\delta^{18}O$ ($^{18}O/^{16}O$) and $\delta^{2}H$ ($^{2}H/^{1}H$), dissolved inorganic and organic carbon concentrations (DIC and DOC) including $\delta^{13}C$ ($^{13}C/^{12}C$), $\delta^{14}C$ ($^{14}C/^{12}C$) in DIC and DOC, and tritium concentrations.

Major ion concentrations were measured in the Geochemistry Lab at the University of Ottawa. Cations were acidified in the lab with nitric acid and measured by Inductively Coupled Plasma

Emission Spectroscopy (Vista-ICP-OES), and anions were measured by ion chromatograph (Dionex ICS-2100).

$\delta^{18}O$ and $\delta^{2}H$ were analyzed by Laser Absorption Spectroscopy (LAS) using a Los Gatos Research (LGR) Liquid Water Isotopic Analyzer (Model LWIA-24d). Measurement precision for hydrogen is ±1 per mil and ±0.25 per mil for oxygen. Results are with respect to Vienna Standard Mean Ocean Water (VSMOW).

Total and dissolved inorganic/organic carbon were first measured by OI Analytical Aurora Model 1030W TIC-TOC Analyzer to determine ppm C, followed by analysis for δ13C (St-Jean, 2003). The TIC-TOC is interfaced to a Finnigan Mat DeltaPlusXP Isotope Ratio Mass Spectrometer for analysis by continuous flow. Data is normalized using three different internal organic standards, with an analytical precision of 2% for carbon concentrations (ppm) and ±0.2 per mil for $\delta^{13}C$. Inorganic carbon exists as carbonic acid (H_2CO_3) bicarbonate (HCO_3^-), and carbonate (CO_3^{2-}). The pH of the water controls the relative abundance of these species. With an average pH of 7.8, bicarbonate (HCO_3^-) is the dominate species of the dissolved inorganic carbon content of the river (Clark and Fritz, 1997).

Tritium activity in water was analyzed by liquid scintillation counting on a Quantulus 1220 low level liquid scintillation counter. Due to the low tritium content of the water, the samples had to be enriched using an electrolytic enrichment method at the University of Ottawa Radiohalide Lab. 250 ml of sample water were deionized using a mixed bed ion exchange resin and shaken for a minimum of 4 hours, and included one duplicate sample. The deionized water was then transferred into electrolytic cells combined with 1 g of sodium peroxide (Na_2O_2) and enriched for a period of 5 days to a final volume of approximately 10 ml. The enriched water was then distilled to remove the sodium peroxide and mixed with UltimaGold LLT™ (low level tritium) cocktail before counting. Counting results were reported in Bq/L (Bq = Becquerel or one nucleus decay per second) and in tritium units (TU), with a limit of detection of 1.1 Bq/L. Water from mid-Holocene glacier ice was used as a blank to calculate instrument detection limit. The standard used in the calibration for Quantulus 1220 is a certified standard SRM 4926E activity 0.0028mCi ^{3}H water from National Institute of Standards and Technology.

Dissolved inorganic and organic carbon was extracted from water as CO_2 then graphitized as a preparation process for ^{14}C analysis on the Accelerator Mass Spectrometer (AMS) at the University of Ottawa Advanced Researched Complex. Iron powder was used as a catalyst to reduce the conversion time of CO_2 to graphite, which takes place under an H_2 environment. Standards of oxalic acid were provided by the University of Ottawa Radiocarbon Lab. Individual analyses are accompanied by their analytical uncertainty.

3.3 Hydrograph Separation

Stream hydrograph separation into baseflow and storm runoff components is the basic tool in determining the components of total discharge from a catchment and water budgets. The principle of hydrograph separation using stable isotopes (oxygen-18 and deuterium) is based on a contrast in the isotopic composition of the basin groundwater with that of other water events (rain water, snow melt, etc.). The groundwater contributing to the basin will have an isotopic composition which reflects a long-term average input value whereas the event waters will have a discrete δ-value somewhere within the range of the mean annual river water. Other components such as stable isotope geochemistry are also expected to vary with the ratio of baseflow to total stream discharge (Hoeg *et al*., 2000; Clark and Fritz, 1997; Klaus and McDonnell, 2013; Carey *et al*., 2012) and can be used in place of oxygen-18 or deuterium.

Traditionally a two component mixing model (composed of the groundwater or baseflow and precipitation or event water) has been used to create a hydrograph, separated into their contributions to total river discharge, based on a mass balance approach:

$$Q_t = Q_p + Q_e$$

$$C_t Q_t = C_p Q_p + C_e Q_e$$

$$F_p = \frac{C_t - C_e}{C_p - C_e}$$

Where Qt is the stream flow, Qp the contribution from pre-event water, Qe the contribution from event water, Ct, Cp, and Ce are the δ values or solute concentrations of stream flow, pre-event water and event water, and F_p is the fraction of pre-event water of total river discharge.

The use of these mixing equations to solve for event and pre-event components of total river discharge rely on several key assumptions (Moore, 1989; Buttle, 1994):

1. The isotopic content of the event and the pre-event water are significantly different.
2. The event water maintains a constant isotopic signature in space and time, or any variation can be accounted for.
3. The pre-event water maintains a constant isotopic signature in space and time, or any variation can be accounted for.
4. Contributions from the vadose (unsaturated zone) must be negligible, or the isotopic content of the soil water must be similar to that of groundwater.
5. Contributions to stream flow from surface storage is negligible.

Early work with two component hydrograph separations showed that soil water can contribute significantly to total river discharge (Kennedy et al., 1986; DeWalle et al., 1988), however one of the major assumptions with a two component hydrograph is that the soil water contribution is negligible or isotopically similar to that of the baseflow component. DeWalle et al. (1988) showed that soil water and groundwater can have a distinct isotopic signal, which renders the previous assumption invalid. This can result in unrealistic component mixtures and necessitated the need for the three component hydrograph separation. To use a three component mass balance approach, either one of the flow components must be known or an additional isotopic tracer used. Since then, a multi component approach to account for additional contributing end-members has been created and employed (Klaus and McDonnell, 2013). The standard mixing equations can now be extended to:

$$Q_t = Q_1 + Q_2 + Q_3$$

$$C_t Q_t = C_1 Q_1 + C_2 Q_2 + C_3 Q_3$$

Most often the two-component mixing model is accepted when there is no sample from deep, old, groundwater. However, in permafrost environments, where temperatures remain well below zero for parts of the year, winter baseflow is entirely supported by taliks providing

passages for intra- and subpermafrost groundwater to the streambed. This groundwater discharge can be the only source of river water in the winter (Woo, 2012).

3.4 Principal Component Analysis (PCA)

Principal component analysis is the mathematical transformation of a data set to help identify correlations within a large set of variables. PCA analysis quantifies the variable interactions by computing the matrix of correlations for the dataset. The matrix of correlations is then decomposed into two matrices by the mathematical tool of eigneanalysis. These two matrices, known as the scores matrix and loadings matrix, provide a means to derive mutually independent axes (dimension) that can describe the data set. These axes, referred to as principal components, are linear combinations of the original variables that arise out of the natural associations among the variables. The idea is to derive a principal component containing most of the total variance in the data set, concentrated into a few derived variables (Meglan, 1992).

Part of the data set was subject to a PCA in order to determine relationships between variables. Only samples taken from the North Klondike River, from January 7th to August 23rd 2014, were involved in the PCA. Variables used include dissolved solutes (calcium, potassium, magnesium, sodium, fluoride, chlorine, sulphate, nitrate), DIC, DOC, $\delta^{13}C$, $\delta^{18}O$, $\delta^{2}H$, and daily mean discharge. The analysis was carried out using XLSTAT, a Microsoft Excel statistical add-in.

4. Results

The results are presented in the following six sections. The first is the temperature record for a given year followed by a given discharge profile, as well as precipitation data for the 2014. The second section contains major ion geochemistry and the third section contains stable isotope data for oxygen-18 and deuterium. The fourth section contains stable and radio-isotope data for carbon. The fifth section contains results from tritium enrichment. The final section contains results from the hydrograph separation.

4.1 Discharge, Temperature, and Precipitation

Temperature was collected at Dawson City Airport for Environment Canada and by the Tombstone Interpretive Center for Environment Yukon. Environment Canada climate data was obtained through the Government of Canada's Historical Climate records and the Environment Yukon data was accessed from the weather station directly. Figure 8 shows discharge, maximum and minimum temperatures, and precipitation recorded in in Tombstone Territorial Park for 2014. Figures 9 through 11 show discharge and temperature profiles for 2012-2014.

Snowmelt is the dominant hydrometric event in subarctic catchments. As such, most streams are characterised by their response to different melting regimes. Church (1974) was the first to classify stream flow regimes according to the primary hydrologic processes and their subsequent hydrographs. The North Klondike River would be considered a subarctic nival (snow-dominated) and spring-fed regime. Characteristics of these regimes include:

(1) snowmelt as a prominent feature,
(2) long stream flow seasons,
(3) frequent increases in summer flow produced by rainfall events,
(4) a low flow period during the winter, maintained by groundwater discharge through taliks in discontinuous permafrost creating a relatively stable stream flow.

The North Klondike River discharge and river valley temperatures are closely related as spring freshet and peak discharge are dependent on temperatures just below or above 0 °C. Peak discharge is often seen in late May, but can be seen as late as June. Peak discharge is an artifact of accumulated snow melt over the winter months and can often be preceded or succeeded by

smaller discharge events. When comparing total annual discharge to that of preceding years, 2014 had ~11% less total annual discharge than 2013, and ~3% less total annual discharge than 2012. 2014 also had a significantly lower spring discharge event, June 19th to July 3rd, compared to that of preceding years. Discharge into September and October shows a familiar decrease in total river discharge as temperatures drop and precipitation begins to arrive as snow.

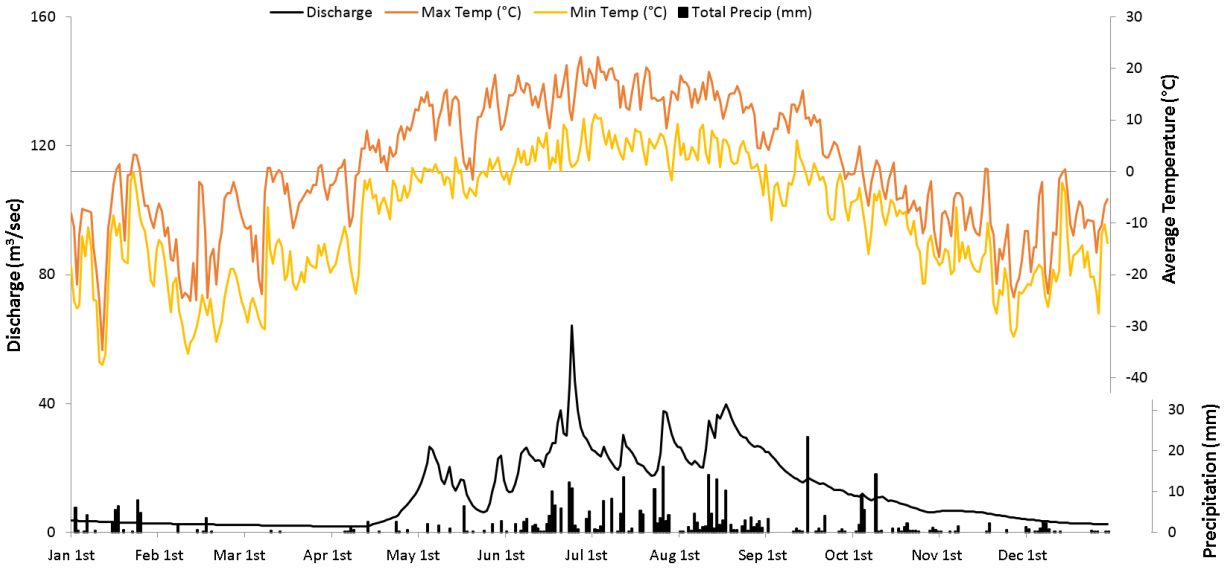

Figure 8 North Klondike total river discharge with precipitation, maximum and minimum temperatures recorded in Tombstone Territorial Park by Environment Yukon, 2014.

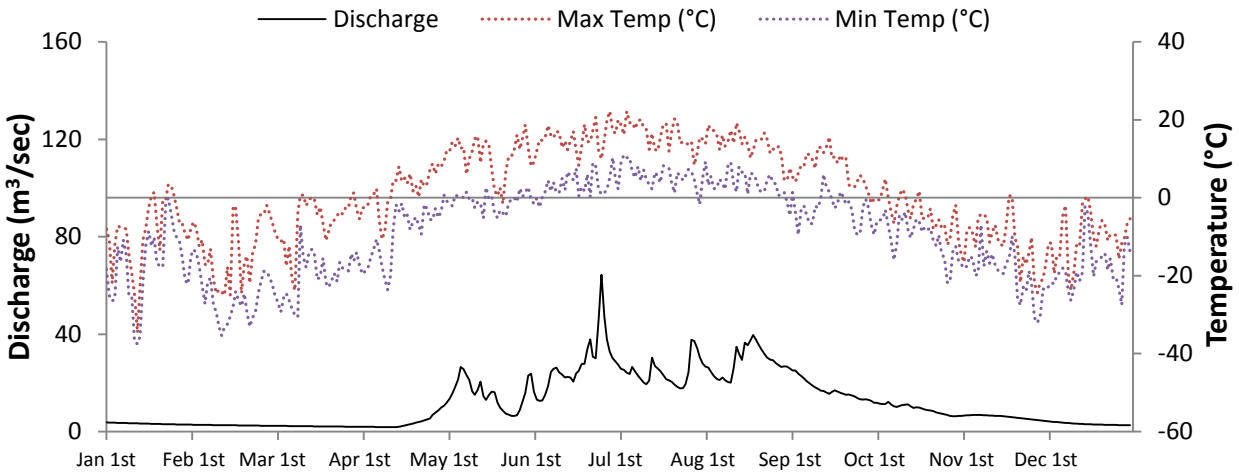

Figure 9 North Klondike total river discharge with maximum and minimum temperatures recorded in Tombstone Territorial Park by Environment Yukon, 2014.

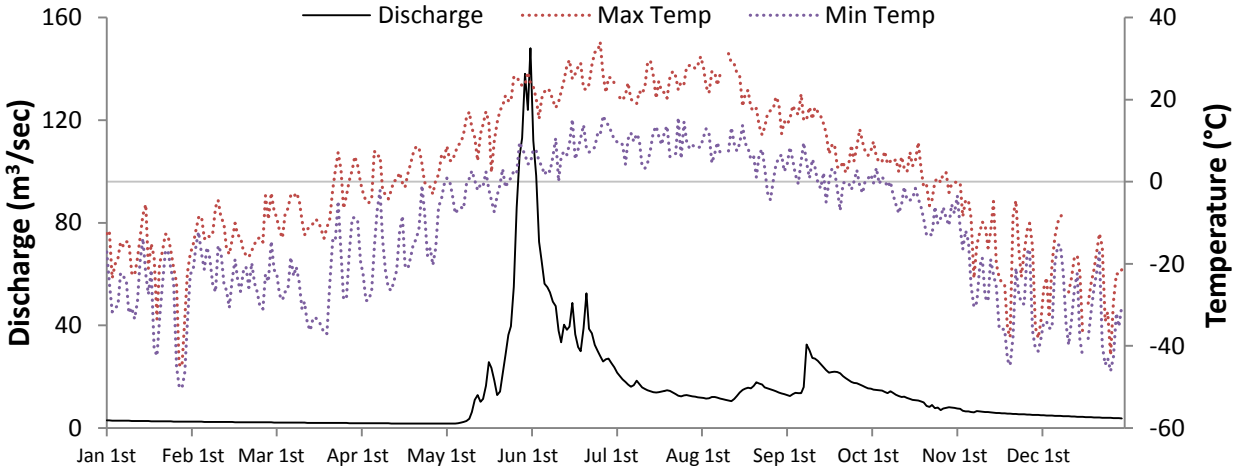

Figure 10 North Klondike River discharge with maximum and minimum temperatures recorded at Dawson City Airport, 2013.

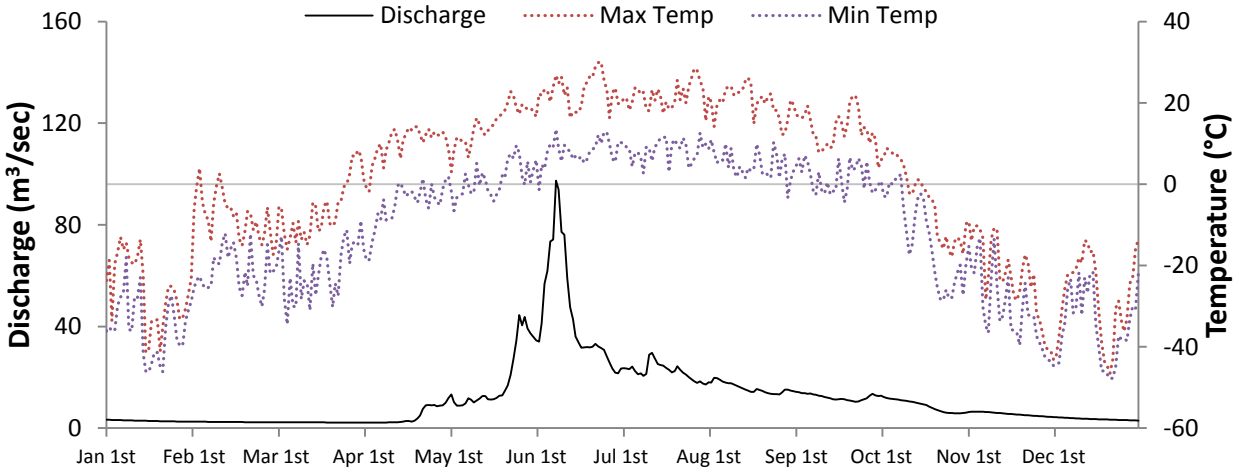

Figure 11 North Klondike River discharge with maximum and minimum temperatures recorded at Dawson City Airport, 2012.

4.2 Major Ion Geochemistry

Of the major cations analyzed, calcium (Ca^{2+}), potassium (K^{+}), magnesium (Mg^{2+}), sodium (Na^{+}), and major anions such as fluoride (F^{-}), chlorine (Cl^{-}), sulphate (SO_4^{2-}), and nitrate (NO_3^{-}) were above the detection limit. Concentrations of bicarbonate (HCO_3^{-}) were calculated according to alkalinity and DIC values for water samples. Results for the North Klondike River are shown in figure 12. Results for the 5 sampled tributaries are shown in table 1.

There are a few observable patterns: ions that dilute with increased flow (Ca^{2+}, Mg^{2+}, Na^{+}, SO_4^{2-}, HCO_3^{-}), and those that tend to increase (K^{+}, F^{-}) or show no general trend (Cl^{-}, NO_3^{-}). Ca^{2+}, Mg^{2+}, Na^{+}, SO_4^{2-} are all ions associated with mineral weathering and are at their highest, followed by a brief spike, prior to river breakup and freshet (April 28th). As snowmelt begins to drain into the river their concentrations begin to gradually dilute and achieve a local minima during peak freshet. As the contribution of snowmelt begins to decline, some of these ions show a tendency to increase to pre-freshet levels, but show a greater variability in late spring and into summer. Ions and constituents that are more biologically active (K^{+}, NO_3^{-}) have a less well defined relationship. Decaying organic matter is most likely the source of nitrate in this basin since the human presence here is minimal and no fertilizer is used anywhere close to the basin (Vitousek*i et al.*, 1997).

There were no observed significant correlati0ons between discharge and dissolved solutes, as seen in other hydrological studies in discontinuous permafrost catchments, such as those performed in the Wolf Creek research basin (Boucher and Carey, 2010; Carey *et al.*, 2012). This could be due to a lack of measurements taken.

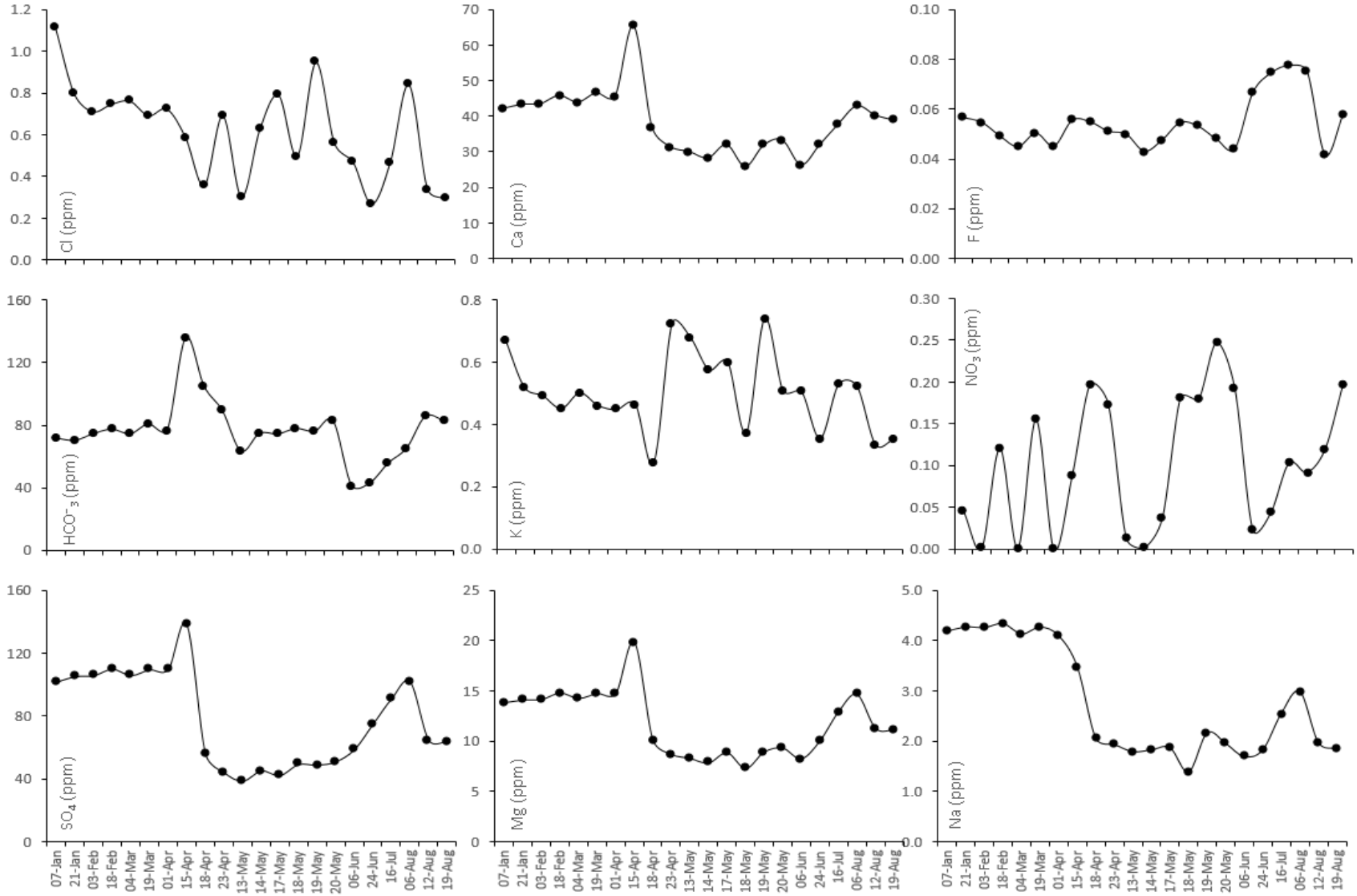

Figure 12 Time series of geogenic solutes in the North Klondike River from January 7th to August 19th, 2014.

Table 1 Geogenic solute concentrations in sampled tributaries of the North Klondike River for 2014.

Tributary	Date Sampled	Ca	K	Mg	Na	F	Cl	SO_4	NO_3	HCO_3
Cairnes Creek	19-May-14	27.48	0.23	8.88	0.45	0.02	0.10	45.52	0.00	n/a
Cairnes Creek	12-Aug-14	33.87	0.13	10.04	0.58	0.02	0.11	53.49	0.12	72.73
Scout Car Creek	17-Apr-14	12.62	0.09	4.16	0.99	0.04	0.23	23.23	0.26	29.48
Scout Car Creek	14-May-14	6.17	0.24	2.04	0.50	0.02	0.35	9.87	0.04	17.54
Scout Car Creek	12-Aug-14	5.62	0.23	1.85	0.37	0.02	0.25	8.42	0.28	12.20
Grizzly Creek	17-Apr-14	14.68	1.74	2.57	0.48	0.04	15.98	5.04	0.31	33.86
Grizzly Creek	14-May-14	13.55	0.78	2.81	0.75	0.08	0.72	18.49	0.14	33.30
Grizzly Creek	12-Aug-14	13.76	0.31	2.50	0.58	0.11	0.21	19.52	0.21	27.51
Black Shale Creek	17-Apr-14	168.52	2.04	94.16	32.27	0.08	2.29	900.96	0.00	183.15
Black Shale Creek	11-May-14	48.92	1.04	32.00	6.92	0.07	0.39	236.01	0.00	47.68
Black Shale Creek	13-Aug-14	113.35	0.88	53.31	9.91	0.08	0.40	476.70	0.41	100.25
Bensen Creek	17-Apr-14	17.33	0.17	5.62	1.08	0.04	0.18	0.00	0.39	50.58
Bensen Creek	13-May-14	9.14	0.23	2.77	0.67	0.03	0.19	13.40	0.00	31.42
Bensen Creek	12-Aug-14	8.83	0.26	2.57	0.59	0.03	0.19	13.16	0.03	20.55

4.3 Oxygen-18 and Deuterium

Precipitation collected at the Dawson City airport during 2013 and 2014 was used to establish a local meteoric water line for the area. Samples were collected after every precipitation event within that interval. The results are shown in figure 13. The equation for the LMWL in Dawson is $\delta^2H = 6.3\delta^{18}O - 35.7$, a slope slightly lower than the GWML, with a slope of ~8. Precipitation collected at Dawson City airport shows similar trends to precipitation collected from Mayo, YT (approximately 180km from the airport) from 1985-1989. This supports the use of precipitation collected from Dawson to be a good approximation of precipitation falling within the North Klondike River valley. $\delta^{18}O$ and δ^2H values in the North Klondike River show distinct seasonal trends. During the winter months, values plot close to the LMWL which is consistent with a groundwater dominated system recharged by precipitation. As the river breaks and with the arrival of spring freshet, isotopic values shift above the LMWL and become slightly depleted. The arrival of summer brings about a shift in $\delta^{18}O$ and δ^2H values back towards the LMWL.

The stable isotopes of oxygen-18 and deuterium were measured at the outlet of the North Klondike River for 2014. Results are shown in Figures 14 and 15. The stream values of $\delta^{18}O$ and δ^2H have a similar behaviour with a few distinct differences. Both show a prominent depletion episode in May which coincides with spring freshet due to the contribution of snow melt which have lower $\delta^{18}O$ values. $\delta^{18}O$ have another depletion event in July, coinciding with maximum river discharge. δ^2H does not show any depletion during maximum discharge. This isotopic response has been observed in other permafrost catchments (Carey *et al.*, 2012), and suggests a mixing of groundwater with snowmelt water. The frequent changes in discharge, from May to June, create a highly variable isotopic signal.

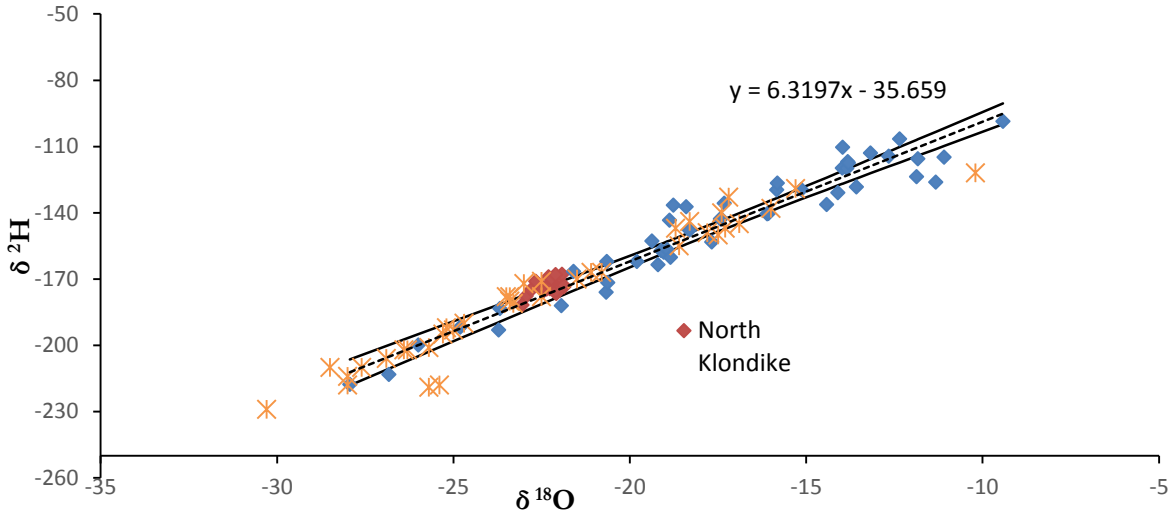

Figure 13 Deuterium and oxygen-18 of rainwater collected at Dawson City Airport (2013-2014) and North Klondike River Water (2014). The dotted black line represents the LMWL at the 95% confidence interval The orange stars represent precipitation collected at Mayo, YT from 1985-1989.

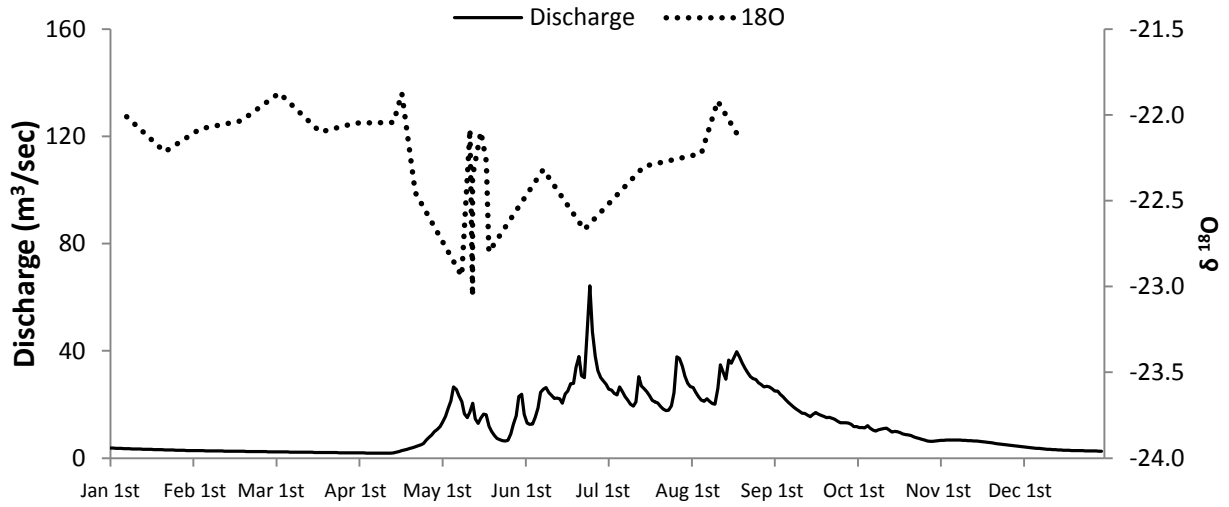

Figure 14 Time series of$\delta^{18}O$ observed at the outlet of the North Klondike River against total river discharge in 2014.

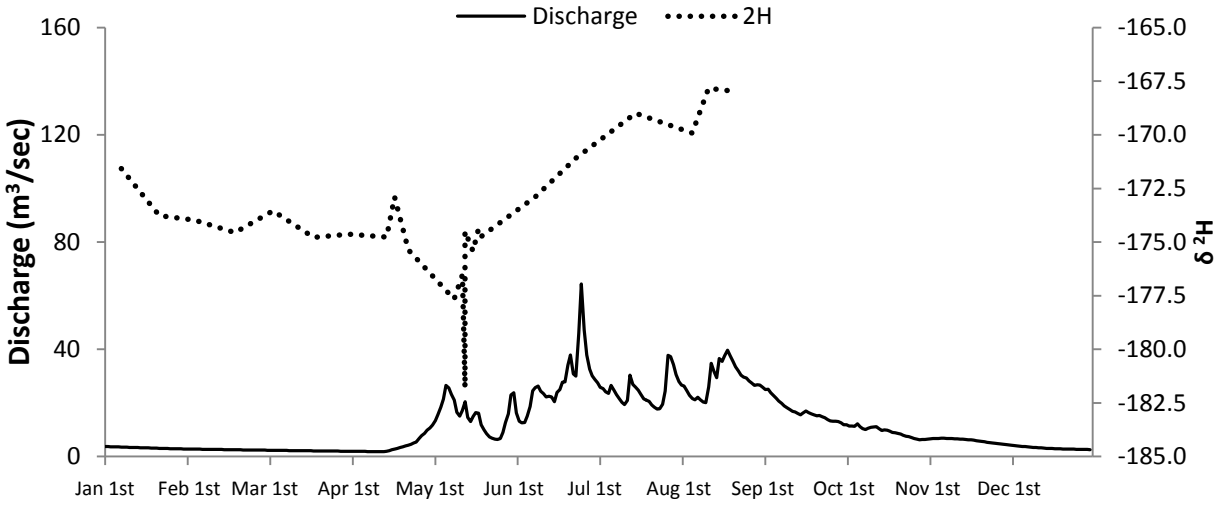

Figure 15 Time series of δ^2H observed at the outlet of the North Klondike River against total river discharge in 2014.

4.4 Carbon

4.4.1 Carbon-13

Figure 16 shows the dissolved inorganic and organic carbon concentrations and $\delta^{13}C$ of DIC/DOC in the North Klondike River over a period of 8 months, which includes major hydrologic events (baseflow, river break, spring freshet, summer flow). DIC and DOC within sampled tributaries for 2014 is shown in table 2.

The concentration of DIC within the North Klondike shows no significant change during the winter months prior to river break and spring freshet. As the river breaks on April 28th, DIC spikes to the largest observed concentration of 25ppm (135 ppm HCO_3^-), before decreasing,. DIC rapidly increases once more in May, before finally decreasing to below pre-river break levels during June. DIC then slowly rises over the summer and into August. $\delta^{13}C$ DIC show no real significant changes throughout the year, except for a small dip in April following river break, and a small peak in June.

The concentration of DOC within the North Klondike River shows no significant change during the winter months prior to river break and spring freshet, with all measured concentrations <1 ppm. The speciation of DOC within the North Klondike is unknown. Following the river break and at the onset of spring freshet, DOC levels begin to rise to their maximum observed concentrations of 8.5 ppm. This rise in DOC has been observed during spring freshet events in other rivers within discontinuous permafrost (Carey, 2003; Carey and Quinton, 2004; Carey and Quinton 2005; Petrone *et al.,* 2006*;* Walvoord and Streigl, 2007; Boucher and Carey, 2010) and rapidly declines as labile carbon is flushed from the catchment (Boucher and Carey, 2010). $\delta^{13}C$ DOC values during the winter months coincide with old carbon, stored within the catchment. With the beginning of spring freshet, $\delta^{13}C$ DOC values shift to those associated with soil carbon.

Table 2 DIC and DOC concentrations within sampled tributaries of the North Klondike River in 2014.

Sample ID	Date	ppm DOC	δ 13 DOC	ppm DIC	δ 13 DIC
Bensen Creek	2014-04-18	0.5	-26.65	9.95	-9.78
Bensen Creek	2014-05-13	2.56	-27.35	6.18	-10.69
Bensen Creek	2014-08-18	1.99	-26.75	4.04	-2.66
Black Shale	2014-04-17	1.55	-25.45	36.03	-5.09
Black Shale	2014-05-11	5.93	-27.49	9.38	-6.2
Black Shale	2014-08-18	0.95	-26.02	19.72	-2.26
Scout Car	2014-04-17	0.48	-27.50	5.80	-7.42
Scout Car	2014-05-14	1.39	-26.82	3.45	-7.2
Scout Car	2014-08-18	1.13	-26.86	2.40	3.86
Grizzly Creek	2014-04-17	2.03	-27.54	6.66	-17.26
Grizzly Creek	2014-05-14	2.87	-26.83	6.55	-8.51
Grizzly Creek	2014-08-18	1.35	-26.62	5.41	-2.54

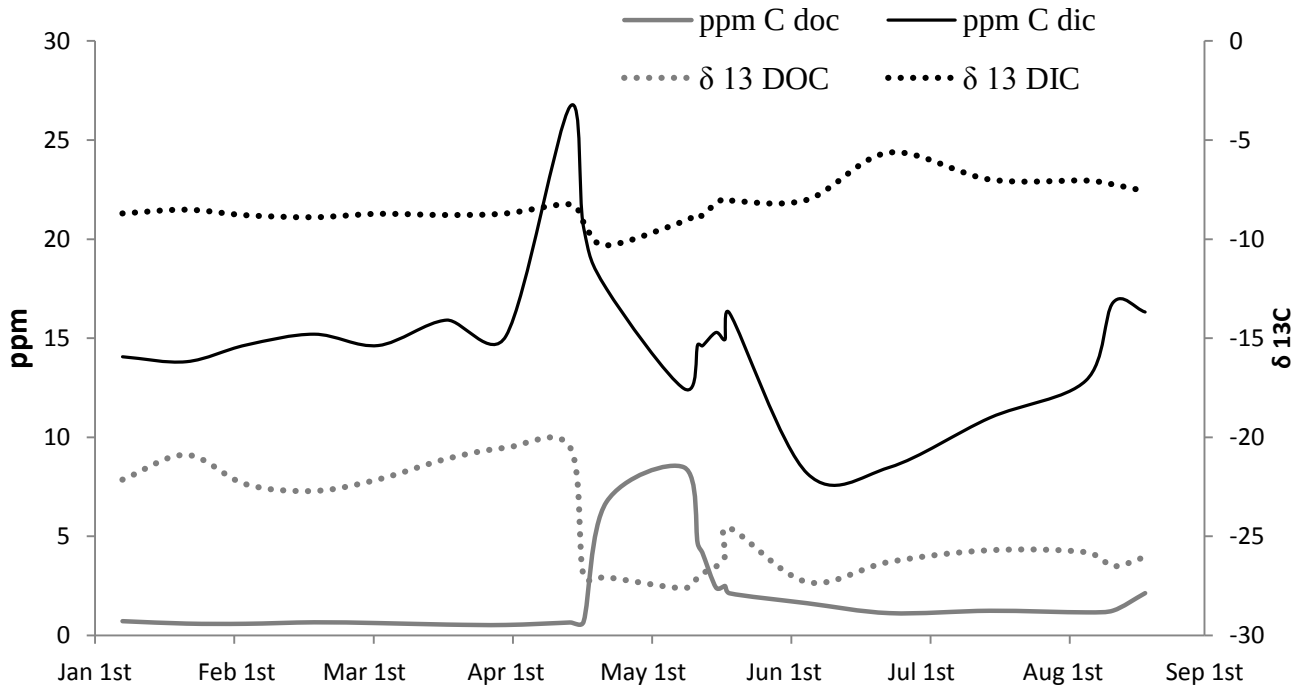

Figure 16 Dissolved carbon content in the North Klondike River from January 7th to August 19th, 2014. Carbon concentrations are expressed as ppm of pure C. Delta C13 is expressed relative to VPDB.

4.4.2 Carbon-14

DIC and DOC Carbon-14 activities were measured in select samples to determine carbon sources and pathways during major hydrologic events, such as baseflow and spring freshet. 15 DIC and 2 DOC samples were measured for ^{14}C; results are reported in table 3. Not all samples could be analysed due to time restraints. DIC shows no change in dates before spring freshet. There is a shift to older inorganic carbon just prior to river break on April 15th that shows a 50% fraction of older carbon. During spring freshet, values shift to modern values containing greater than 70% modern carbon. ^{14}C activities in DOC show that older carbon dominates baseflow, with an influx of modern carbon during and then after the river breaks, consistent with other studies (Raymond *et al.*, 2007; Aiken *et al.* 2014). These changes in ^{14}C also coincide with changes in $\delta\ ^{13}C$ values that indicate a greater contribution of modern carbon.

Table 3 Carbon-14 activities for select DIC and DOC samples from the North Klondike River in 2014. ^{14}C DIC is representative of baseflow, river break, and spring freshet. ^{14}C DOC is representative of baseflow and spring freshet. Results are reported as both $^{14}C/^{12}C$ and in years before 1950.

Date	$^{14}C/^{12}C$	±	Years Before 1950	±
DIC				
07-Jan-14	0.61	3.16E-03	3955	41.6
21-Jan-14	0.61	2.30E-03	3924	30.0
03-Feb-14	0.63	2.20E-03	3710	29.0
18-Feb-14	0.60	2.96E-03	4136	39.8
04-Mar-14	0.62	2.20E-03	3870	29.0
19-Mar-14	0.61	3.07E-03	3960	40.4
01-Apr-14	0.62	2.95E-03	3842	38.3
15-Apr-14	0.49	2.54E-03	5673	41.3
18-Apr-14	0.65	3.24E-03	3490	40.2
23-Apr-14	0.70	3.99E-03	2877	45.8
10-May-14	0.77	2.50E-03	2141	27.0
13-May-14	0.73	4.16E-03	2489	45.5
14-May-14	0.78	2.70E-03	2035	27.0
19-May-14	0.74	2.60E-03	2454	29.0
20-May-14	0.73	3.85E-03	2522	42.3
DOC				
18-Feb-14	0.56	3.51E-03	4722.9	50.7
23-Apr-14	0.94	4.81E-03	506.0	41.2

4.5 Tritium

8 water samples were analyzed for tritium concentrations in the North Klondike River for the year of 2014. Results are shown in table 4 and figure 17. Tritium concentrations are reported in Becquerel's per litre (Bq/L) and in tritium units (TU). June 9th, 2014 had a much higher error due to liquid scintillation counting of a small volume of sample, at values just above background. The highest tritium concentrations were found at the beginning of May, with the lowest values observed a week later. The higher the tritium content in the water, the greater the contribution of younger water to total stream discharge. Following the lowest tritium concentration on May 19th, tritium values continue to rise until August. Average tritium activity within the North Klondike River was 10.8 TU.

Table 4 Tritium activity in the North Klondike River for 2014.

Date	TU	±	Bq/L	±
21-Jan-14	12.03	0.67	1.43	0.08
3-Feb-14	7.77	1.07	0.92	0.13
4-Mar-14	8.29	1.19	0.98	0.14
18-Apr-14	10.16	1.48	1.21	0.18
13-May-14	17.72	1.12	2.11	0.13
19-May-14	6.68	1.15	0.79	0.14
9-Jun-14	10.52	4.56	1.25	0.54
6-Aug-14	13.37	1.53	1.59	0.18

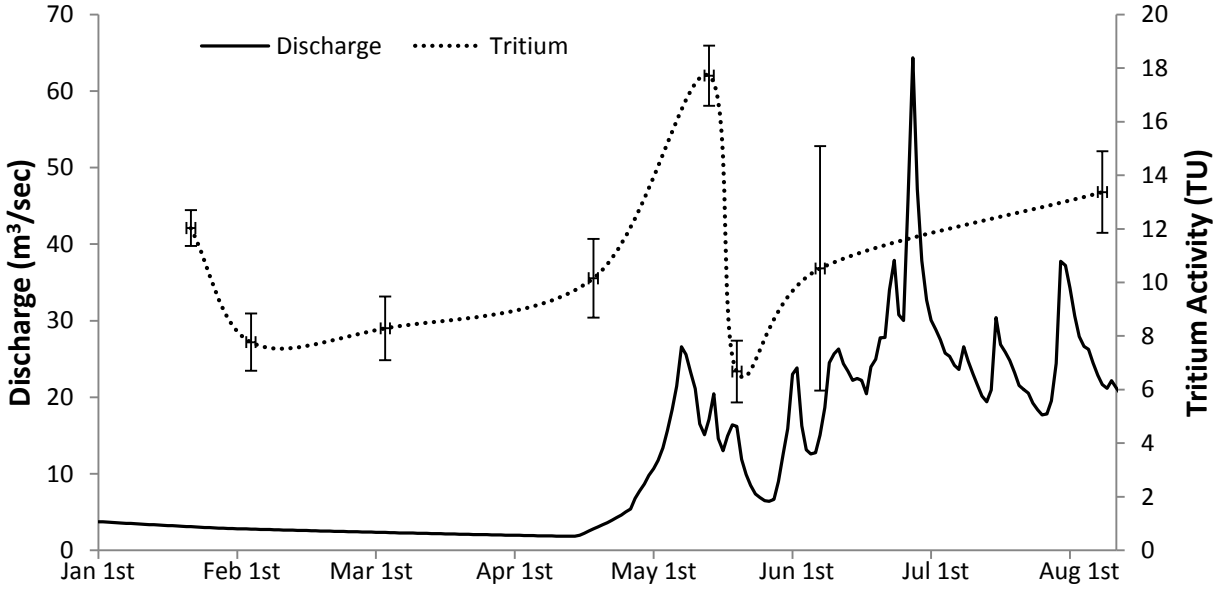

Figure 17 Measured tritium activity (expressed as tritium units or TU) and total river discharge in the North Klondike river, 2014.

4.6 Hydrograph Separation

The main objective of this thesis was to identify seasonal groundwater contribution to total river discharge within the North Klondike River and potential flow pathways. Due to the muted maximum discharge event and the inability to sample active layer discharge, a three component hydrograph was determined to be unsuitable. A two component hydrograph was utilized instead to model mixing of the two dominant hydrological components, groundwater (baseflow), and precipitation/snowmelt or runoff.

The stream water before the river breaks is deemed to be the most representative of baseflow. The other component is precipitation, which was collected from the Dawson City Airport. Although not within the river basin, this was the closest location and is assumed to be a good geochemical representation of precipitation falling in this area. Soil water could not be extracted and therefore measured for solutes. Baseflow or groundwater shows the highest concentration of dissolved solutes, whereas precipitation shows the lowest concentration of dissolved solutes.

Four different solutes were used (SO_4, Mg, Ca, Na) for the two-component hydrograph. Solutes were chosen according to the difference in their concentrations between groundwater and precipitation, as well as their capacity to move through the system without being chemical altered or removed. The results are shown in figures 18 through 21. This simple mixing model ($C_tQ_t = C_pQ_p + C_eQ_e$) suggests that despite a variable discharge during the winter months, groundwater is still the most significant contributor, supporting over 95% of total river discharge. The drop in groundwater contribution during April is consistent with the river break, and the onset of spring freshet. In some iterations, surface runoff and precipitation becomes the dominate component from mid-April to late-May, contributing over 50% of total river discharge. Between all mixing models, surface runoff accounts for between 30 – 60% of total river discharge during spring freshet and into summer. If not already, groundwater then once again becomes the dominate component by late June, and its contribution increases until August. The rise in runoff during August coincides with large rainfall and storm events, which is also seen as peaks within the stream hydrograph.

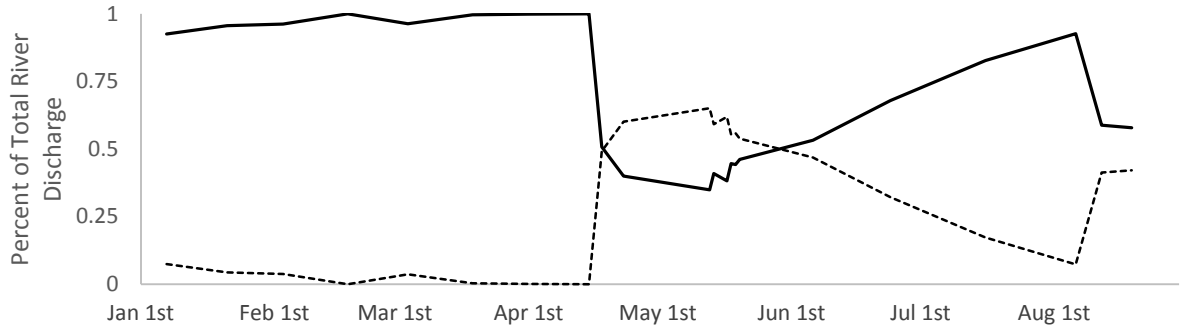

Figure 18 A 2-component hydrograph separation using SO_4, representing the relative contribution of groundwater (solid black) and runoff (dotted black) to total river discharge for 2014.

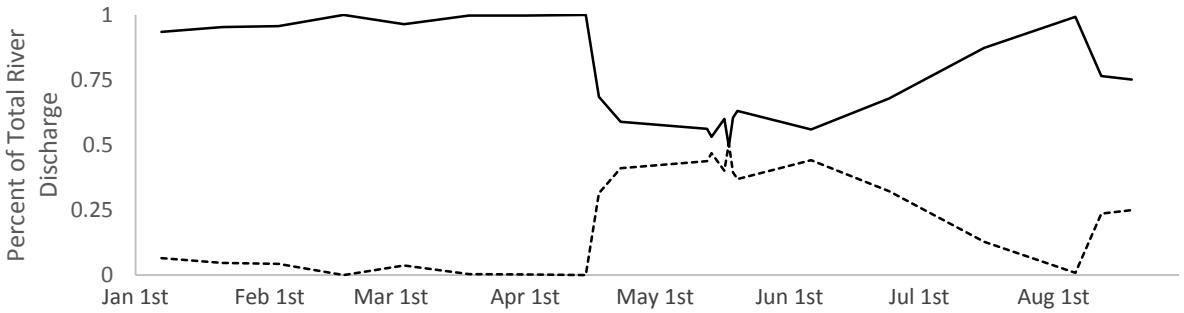

Figure 19 A 2-component hydrograph separation using Mg, representing the relative contribution of groundwater (solid black) and runoff (dotted black) to total river discharge for 2014.

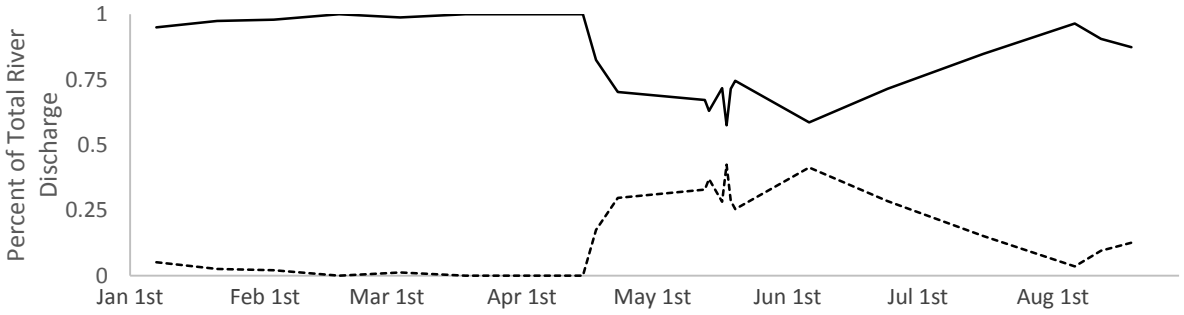

Figure 20 A 2-component hydrograph separation using Ca, representing the relative contribution of groundwater (solid black) and runoff (dotted black) to total river discharge for 2014.

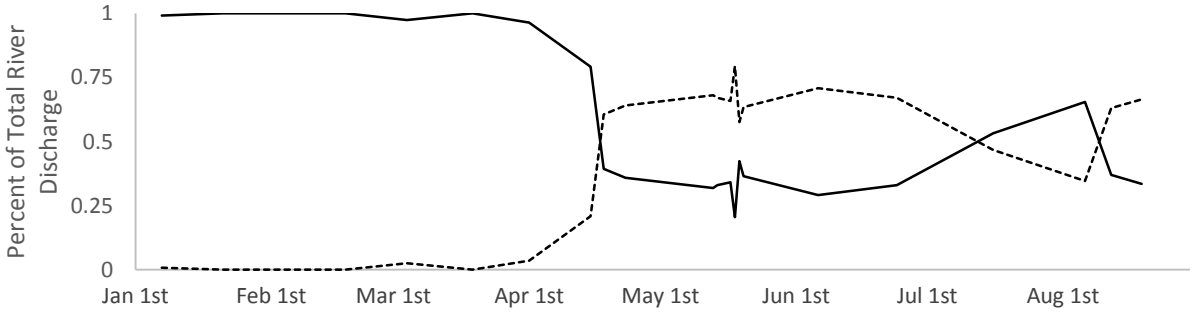

Figure 21 A 2-component hydrograph separation using Na, representing the relative contribution of groundwater (solid black) and runoff (dotted black) to total river discharge for 2014.

5. Discussion

This discussion is presented in 7 sections, which will expand on the data presented in previous sections.

5.1 North Klondike River discharge

The average total river discharge during winter months preceding river break and spring freshet is ~ 2.7 m^3/sec. Localized warming events show a thinning of the snow pack (Figure 22), but no changes in winter baseflow. The North Klondike River broke on approximately April 28th, 2014, followed by the beginning of spring freshet and the contribution of snowmelt. Drops in temperature to at or below 0°C show a delayed decrease in total river discharge. Peak discharge is not seen until June, when minimum temperatures remain above 0°, coupled with summer rain events. Following peak discharge, total river discharge begins to decrease towards baseflow unless supplemented by summer and fall rain storm events.

Sub-arctic regions have a high percentage of precipitation arriving as snow on the ground, lasting from October-November to March-April (Woo, 2012). Compared with temperate latitudes, the arrival of snowmelt in subarctic regions or high mountains can be delayed by weeks or even months. In the case of the North Klondike River valley, it is both subarctic with high mountains. This delay in melt is caused by the persistence of coldness in the atmosphere, and the high albedo of the snow cover which reflects much of the incoming solar radiation. This can create a considerable time lag between the warming of the air, the dissipation of the coldness in the snow, to the generation of melt and finally to the delivery of meltwater to the river. The duration of this melt can also be prolonged if the terrain covers a range of elevations (Woo, 2012). This could explain the time lag seen in the North Klondike River hydrograph of previous years; where discharge increased with rising temperatures, but did not spike to maximum levels until joined by the snowmelt.

At high latitudes, the low angle of incoming solar radiation can also have an effect on snowmelt. This low sun angle combined with north-facing slopes can result in very low direct solar radiation, even with prolonged days. This can be further exaggerated by the presence of rugged topography and the casting of shadows. Ground cover also plays a role in snow melt generation. The North Klondike river valley contains a land cover distribution typical to that

of northwestern North America boreal zones, with forests dominating lower elevations and the valley floor, with shrubs, lichen, and moss dominating at higher elevations (Kojima, 1996). These changes in ground cover can have an effect on melt rates, with more intense melting in open sites than in the forests (Woo, 2012).

Much of the change in total river discharge can be explained as the influx of precipitation, as either snowmelt or rain. There is much debate about the specific pathways of melt water and its specific contribution to total river discharge. It has been suggested that surface material is unsaturated, and requires the establishment of a near surface water table before runoff can be conveyed to the stream (Carey and Quinton, 2003). Others have proposed that catchment soils are already saturated with pre-event or old water, and this influx of melt water displaces pre-event water (Boucher and Carey, 2010) which dominates the freshet hydrograph, although the mechanism and runoff pathways are still unclear.

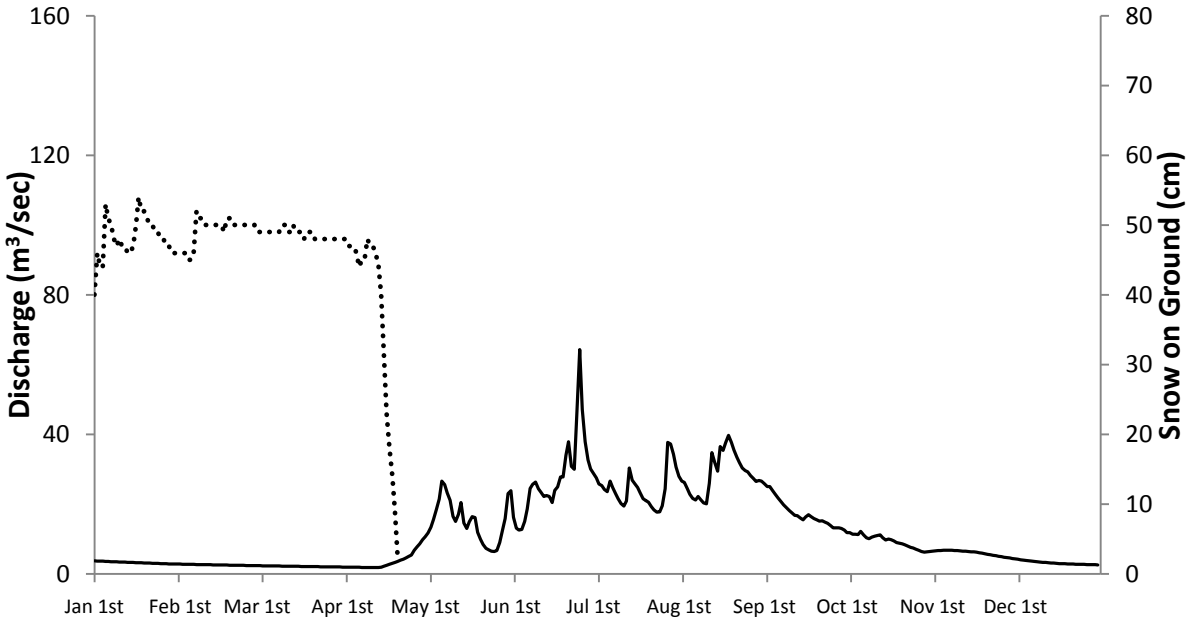

Figure 22 Total river discharge for the North Klondike River and snow cover on ground in cm recorded at Dawson City airport for 2014.

5.2 Major Ion Geochemistry

Stream flow chemistry provides a means to assess flow pathways within the catchment. Geogenic ions such as Mg^{2+}, Ca^{2+}, Na^{+}, and SO_4^{2-} are present in high concentrations during the winter, when stream flow is maintained by groundwater discharge. Biologically active

ions such as K^+ are more abundant in surface-organic soils when surface runoff and active layer water begins contributing to total stream discharge. Total river discharge remains consistent prior to river break (April 28th), and subsequently geogenic ions show no significant change in concentration.

Before the river breaks on April 28th, concentrations of Mg^{2+}, Ca^{2+}, and SO_4^{2-} increase rapidly before decreasing to below pre-event levels. This increase in solutes are likely a result of temperatures approaching 0°C, initiating localized snowmelt and groundwater discharge. Following this increase, geogenic solutes are most likely being diluted by snowmelt and runoff, which contain very low levels of these solutes. Unlike the other solutes, Na^+ does not show a spike in concentrations during this event. This initial spike in solutes is hypothesized to be uneven snowmelt within the basin, triggering a surge in groundwater from specific tributaries. Black Shale Creek contains the highest concentration of dissolved solutes compared to all other sampled tributaries and even the North Klondike River itself. Black shale creek also has different land cover conditions compared to the rest of the valley, as it sits at or above the tree line in the northern most reaches of the catchment. Shale commonly contains minerals such as gypsum, and muscovite, and are most likely responsible for the very high concentrations of weathering ions compared to the North Klondike and other tributaries. Soils are capable of transmitting water during melt, even at 0°C with no re-freezing occurring (Quinton and Marsh, 1999), so the potential for groundwater recharge and subsequent discharge exists even when the ground is frozen.

By means of an exercise in solute flux (ie. weighting the percent contribution of each watershed to total stream solute flux as a function of individual watershed size) we can estimate the individual tributary contribution of solutes to total river solute concentrations. As alluded to above, Black Shale Creek contains the highest concentrations of all solutes within sampled tributaries. See table 1 for solute concentrations within each tributary sampled. We hypothesize that snow melting within the Black Shale Creek basin triggered an increase in supra-permafrost groundwater stored within the Black Shale Creek basin. Solutes briefly increased in concentration, before the other major tributaries began melting and diluting the signal from Black Shale Creek. This is further supported by K:Ca ratios (Figure 23), which increase with near-surface flow and decrease with slower subsurface pathways (Elseenbeer*et*

al., 1995). K:Ca ratios do not increase until April 23rd, which coincides with a rise in DOC. Similar patterns are seen in other permafrost basins (Carey, 2003; Boucher and Carey, 2010), which show a rise in K:Ca and DOC, prior to spring freshet.

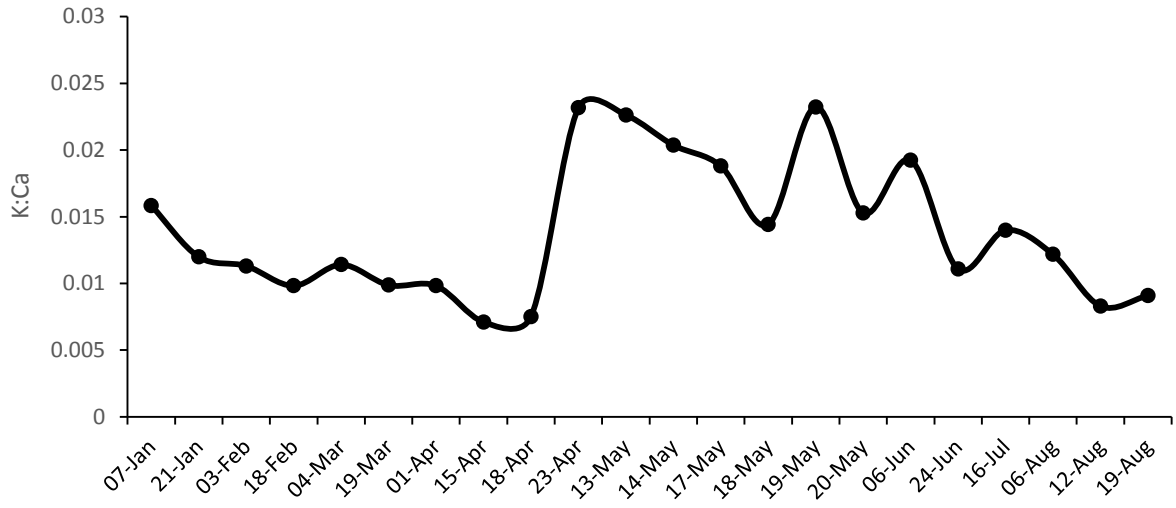

Figure 23 Time series of Potassium-Calcium ratios within the North Klondike River January 7th to August 19th, 2014.

Principal component analysis was used to help establish and interpret trends within the data. The PCA only used data from the North Klondike River, and excluded all tributaries and precipitation samples. Summary statistics are presented in table 5, and the correlation matrix used in the PCA is presented in table 6. From the correlation matrix, loading factors were calculated and presented in table 7. Factor 1 accounts for 39% of the total variance, factor 2 accounts for 23% of the total variance, and factor 3 accounts for 15% of the total variance. Combined, we can account for approximately 77% of the total variance between samples. Factor1can be interpreted as groundwater and is characterised by discharge, calcium, magnesium, sodium, sulphate, and organic carbon. This interpretation is consistent with observed geogenicsolute levels during the winter months and the unique organic carbon profile (very low DOC and enriched $\delta^{13}C$). Oxygen-18 and deuterium are not coupled with factor 1, which is unusual if groundwater is being recharged by precipitation. This uncoupling between ^{18}O and ^{2}H could be a result of chemical interactions below ground, shifting isotopic values off the LMWL. Factor 2 and 3, could be interpreted as precipitation and soil water. The soil zone is a significant source of DIC and depleted $\delta^{13}C$, which enters the river as runoff from

subsurface flow. Nitrate concentrations are barely above detection limit, but could be indicative of subsurface flow as nitrate is a product of biodegradation.

Table 5 Summary statistics for the 22 water samples taken from the North Klondike River in 2014.

Variable	Minimum	Maximum	Mean	Std. deviation
Ca	25.754	65.429	38.312	9.028
K	0.275	0.740	0.503	0.126
Mg	7.303	19.815	11.721	3.236
Na	1.377	4.338	2.764	1.111
F	0.042	0.078	0.054	0.010
Cl	0.266	1.116	0.617	0.227
SO_4	38.756	138.404	78.152	30.055
NO_3	0.000	0.247	0.101	0.080
HCO_3	41.523	135.642	76.245	19.237
DIC	8.168	26.684	14.999	3.784
^{13}C DIC	-10.310	-5.630	-8.277	0.964
DOC	0.525	8.480	2.051	2.142
^{13}C DOC	-27.620	-20.490	-24.669	2.549
Discharge	2.860	20.500	8.562	4.466
^{2}H	-181.774	-167.829	-173.580	3.209
^{18}O	-23.055	-21.872	-22.264	0.332

Table 6 Factor loadings for the first three calculated factors, accounting for 75% of the total variance.

Variable	Factor 1	Factor 2	Factor 3
Ca	**0.935**	0.093	0.168
K	-0.164	**-0.547**	-0.495
Mg	**0.945**	0.190	-0.036
Na	**0.889**	-0.070	-0.400
F	-0.110	**0.716**	-0.307
Cl	0.452	-0.367	-0.492
SO_4	**0.924**	0.254	-0.200
NO_3	0.021	0.121	**0.701**
HCO_3	0.496	-0.401	**0.732**
DIC	0.496	-0.401	**0.732**
^{13}C DIC	-0.160	**0.908**	0.033
DOC	**-0.663**	**-0.532**	-0.012
^{13}C DOC	**0.925**	-0.052	-0.188
Discharge	**-0.630**	**0.616**	0.190
^{2}H	0.198	**0.838**	0.118
^{18}O	**0.631**	0.275	0.082

Table 7 Correlation matrix for 22 North Klondike River water samples (January to August, 2014).

Variables	**Ca**	**K**	**Mg**	**Na**	**F**	**Cl**	**SO4**	**NO3**	**HCO3**	**DIC**	**^{13}C DIC**	**DOC**	**^{13}C DOC**	**Discharge**	**^{2}H**	**^{18}O**
Ca	**1**															
K	-0.203	**1**														
Mg	0.970	-0.172	**1**													
Na	0.739	0.030	0.826	**1**												
F	-0.038	-0.117	0.112	-0.103	**1**											
Cl	0.257	0.586	0.334	0.593	-0.087	**1**										
SO_4	0.888	-0.203	0.966	0.875	0.194	0.361	**1**									
NO_3	0.068	-0.185	-0.043	-0.279	-0.057	-0.042	-0.151	**1**								
HCO_3	0.593	-0.162	0.406	0.146	-0.466	0.044	0.231	0.439	**1**							
DIC	0.593	-0.162	0.406	0.146	-0.466	0.044	0.231	0.439	1.000	**1**						
^{13}C DIC	-0.031	-0.405	0.037	-0.238	0.637	-0.351	0.090	0.184	-0.398	-0.398	**1**					
DOC	-0.555	0.567	-0.627	-0.566	-0.269	-0.197	-0.707	-0.185	-0.089	-0.089	-0.385	**1**				
^{13}C DOC	0.808	-0.070	0.845	0.914	-0.138	0.487	0.878	-0.101	0.317	0.317	-0.165	-0.606	**1**			
Discharge	-0.434	-0.194	-0.434	-0.665	0.410	-0.544	-0.452	0.190	-0.391	-0.391	0.702	0.206	-0.642	**1**		
^{2}H	0.298	-0.376	0.343	0.064	0.492	-0.185	0.318	0.228	-0.141	-0.141	0.676	-0.496	0.066	0.463	**1**	
^{18}O	0.580	-0.222	0.593	0.518	-0.080	0.129	0.578	0.148	0.175	0.175	0.057	-0.436	0.507	-0.190	0.504	**1**

5.3 Seasonal Carbon Flux

In the North Klondike River, baseflow or groundwater is characterised by moderate levels of DIC, with an average bicarbonate concentration of 75 ppm and relatively enriched $\delta^{13}C$ values. DOC values remain very low, averaging 0.6 ppm of organic carbon and relatively enriched $\delta^{13}C$ values. Spring freshet is characterised by an initial icnrease in DIC of 135 ppm bicarbonate before quickly decreasing, while the $\delta^{13}C$ values remain unchanged. DOC follows the increase in DIC, rising to a yearly maximum of 8.5 ppm organic carbon, with $\delta^{13}C$ values shifting to that of modern carbon. Summer flow is characterised by a similar bicarbonate concentration to baseflow, slightly enriched $\delta^{13}C$, and a gradual decline in DOC concentrations.

There is a considerable difference in carbon export between ice covered conditions, spring freshet, and summer. Figures 24 and 25 show dissolved inorganic and organic carbon export within the North Klondike River in 2014, expressed as mg of C per second. Dissolved inorganic carbon export within the North Klondike River basin was anywhere between 0.04 milligrams of carbon per sec (mg C/sec) to a maximum of 0.33 mg C/sec. Dissolved organic carbon export within the North Klondike River basin was anywhere between 0.001 mg C/sec to a maximum of 0.08 mg C/sec. Increases in dissolved inorganic carbon flux are consistent with increases in discharge, especially during the winter months. Dissolved organic carbon shows only a few distinct increases in carbon export, with the maximum values during spring freshet.

The highest concentration of DIC occurs on April 15th, and shares a similar pattern to other measured geogenic solutes. This increase precedes river break by almost a week, when dissolved solutes will reach their lowest levels. This increase in DIC is hypothesized to be attributed to the Black Shale Creek melting event, with melt water triggering an increase in groundwater discharge before melt water from the entire basin could dilute solutes below their baseflow concentrations. The $^{14}C/^{12}C$ faction decreases during this spike in DIC, which is consistent with the hypothesized localised increase in discharge from Black Shale Creek. This spike in DIC is accompanied by geogenic solutes, characteristic of groundwater containing older inorganic carbon.

Following spring freshet, $\delta^{13}C$ values of DIC remain close to baseflow levels, which are characteristic of interactions with rocks below ground of a closed, or partially closed system. DIC has a $^{14}C/^{12}C$ fraction of 0.6 during baseflow, which increases to 0.7 after spring freshet. This increase in modern inorganic carbon could be a result of increased supra-permafrost groundwater flow from within the active layer as well as the beginning of primary productivity and biodegradation of organics (Mohammadzadeh and Clark, 2008). The other significant change in DIC is seen on June 6th. This decrease in DIC is concurrent with an increase in runoff seen in the 2-component hydrograph separation, and hypothesized as precipitation combined with snowmelt from higher elevations.

During baseflow there are no significant changes in DOC concentrations or in $\delta^{13}C$ values. $\delta^{13}C$ values are characteristic of old carbon stored within the catchment, with a large shift to modern values at the onset of spring freshet. Organic carbon undergoing biodegradation has been shown to be enriched in $\delta^{13}C$ (Mohammadzadeh and Clark, 2008). This organic carbon could be released as a weathering product from the surrounding geology, specifically within Black Shale Creek, which contains the highest DOC concentrations (table 1). Shale has the capacity to adsorb meaningful amounts of dissolved organic compounds, and can be preserved in burial (Kennedy *et al*, 2002). Evidence for old carbon stored within the catchment is further supported by organic^{14}C activities (Figure 26), which show a 0.56 fraction of $^{14}C/^{12}C$ during baseflow. During spring freshet, this fraction changes to 0.94 of $^{14}C/^{12}C$, representing a significant fraction of modern carbon. This input of organic carbon is a product of snowmelt and runoff in surface and near surface pathways, characterised by a rise in K:Ca.

DIC and DOC for the sampled tributaries are shown in table 1. As mentioned before, an early melting event is thought to be responsible for this spike in geogenic solutes. DOC concentration within Black Shale Creek and groundwater are very low, and no increase in DOC is observed during the solute spike on April 15th. This lends further support to an early limited melting event within Black Shale Creek, increasing groundwater discharge from the tributary without stimulating near surface flow.

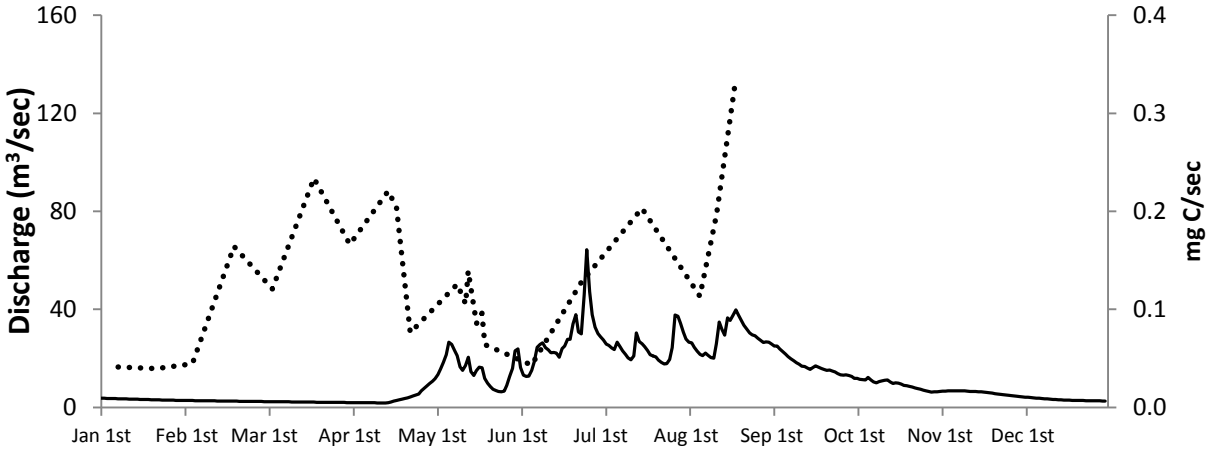

Figure 24 Time series of dissolved inorganic carbon (DIC) export in the North Klondike River in 2014.

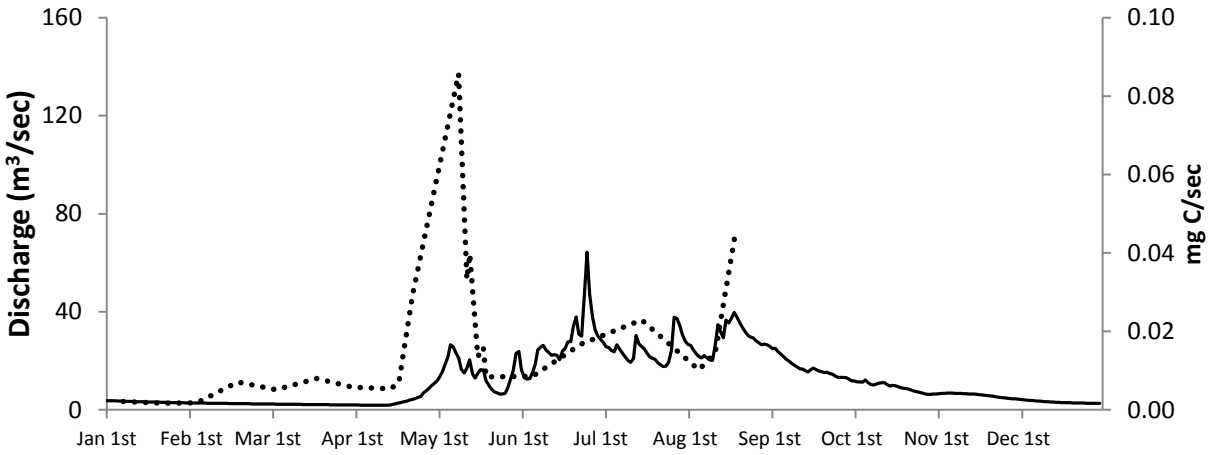

Figure 25 Time series of dissolved organic carbon (DOC) flux in the North Klondike River in 2014.

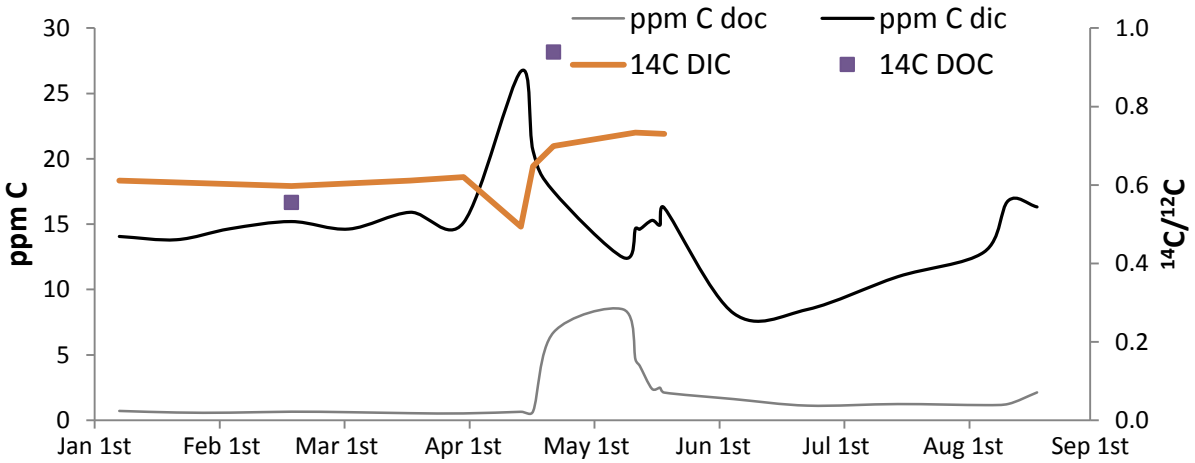

Figure 26 Annual carbon flux in the North Klondike River for the year of 2014. Concentrations of carbon are expressed as ppm of pure C. Carbon-14 activities are expressed as a fraction of $^{14}C/^{12}C$.

5.4 Oxygen-18 and Deuterium

While dissolved ions provide information on flow pathways that water takes within the catchment, stable isotopes provide information on source water and recharge conditions. In most years, snowmelt is the dominant hydrochemical and hydrological event in subarctic permafrost catchments. ^{18}O and ^{2}H within the North Klondike River show more depleted values compared to recorded precipitation values, especially ^{18}O which plots on the left side of the LMWL.

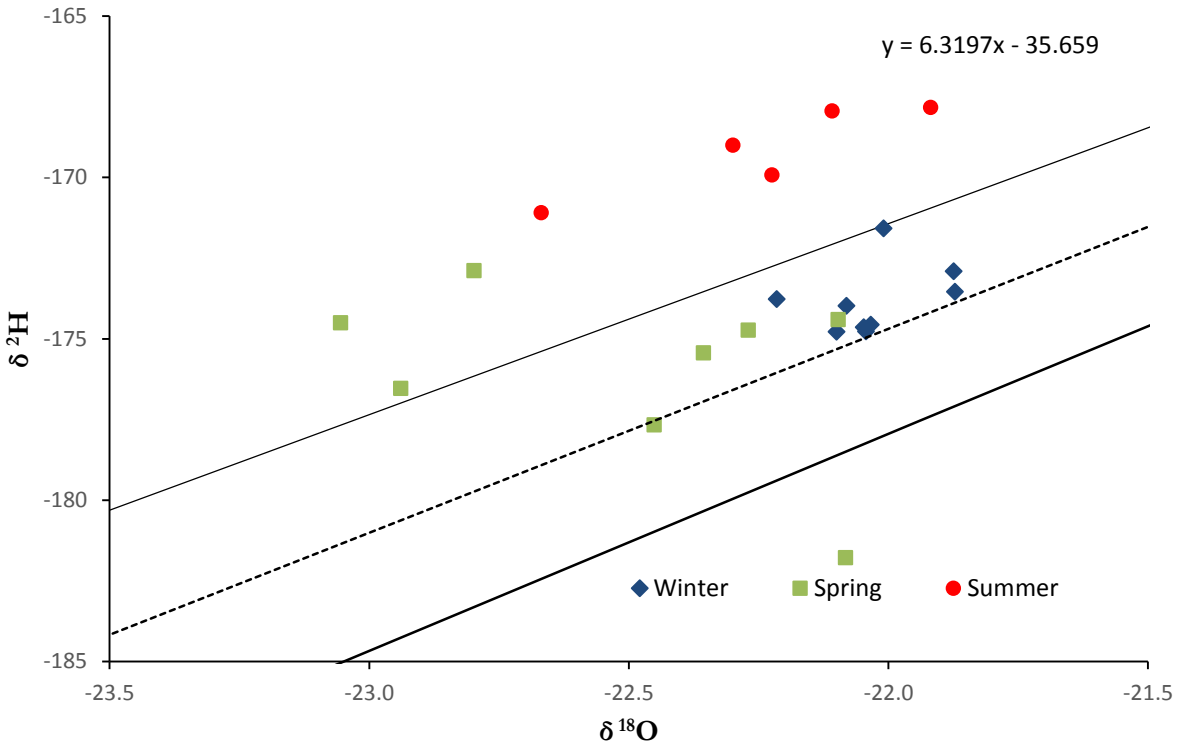

Figure 27 Seasonal variation in oxygen-18 and deuterium within the North Klondike River for 2014 plotted next to the LMWL established at Dawson City airport.

Water from the North Klondike River (Figure 27) shows a seasonal variation over a period of 8 months, with a general depletion of ^{18}O in the spring months (associated with snowmelt) and an enrichment during the winter months (groundwater only). Winter baseflow plots very closely along the local meteoritic water line (LMWL), and not until April and May does the water begin to deviate from the LMWL. It has been observed previously, in varying climates, that the initial snow melt shows a more depleted ^{18}O value followed by increasingly higher values throughout the melting event (Taylor, *et al.* 2002). This water does not show any significant effects of evaporation. Anderson *et al* (2005) constructed a local evaporation line

(LEL) from lakes in the Yukon, and defined a LEL with a slope of ~4. The LEL has a lower slope than both the LMWL and GWML due to diffusion controlled isotopic fractionation during evaporation causing greater ^{18}O-^{16}O separations than ^{2}H-^{1}H. Furthermore, water undergoing evaporation would need to plot on the other side of the LMWL. Furthermore, discharge values cluster close to the mean and are highly attenuated as they do not show the same spread as precipitation. North Klondike River waters also plot on the low end of the LMWL, which is concurrent with winter precipitation, suggesting that recharge is occurring from snowmelt. Since there is no isotopic evidence of significant evaporative loss, water would then be removed from the system as transpiration.

5.5 Water balance and carbon export

Using the total volume of annual river discharge and annual precipitation, it is possible to estimate the annual water balance (precipitation, runoff, rainfall interception, and transpiration) within the North Klondike River valley. Taking this a step further, by estimating water use efficiency for photosynthesis, we can approximate the sum of carbon fixation and CO_2 emissions within the basin. Published water use efficiencies for Canadian boreal forests are between 4.39 and 5.57 moles C per 1000 moles H_2O (1 mole C per 180 moles H_2O or 1 mole C per 228 moles H_2O) (Brummer *et al.*, 2012). Rainfall interception values for boreal forest were established by Grelle *et al.,* in 1997, and are a measure of precipitation that does not contribute to primary productivity or total river discharge. The percentage of boreal forest land cover within the catchment was estimated using satellite imagery. Table 8 is a summary of water balance and total carbon (inorganic and organic) export within the catchment for 2014.

Table 8 Water balance and total carbon export for the North Klondike River basin from January 1st to December 2nd 2014.

Total River Discharge (m^3)	2.87×10^8
Total Precipitation in basin (m^3)	3.95×10^9
Rainfall interception (m^3)	1.1×10^9
Contribution of precipitation to total river discharge	10%
Average water use efficiency (moles of H_2O per mole C)	

	204	±	24
Total carbon production (g C/m^2)	10.2	±	1.5
Carbon emitted or sequestered (g C/m^2)	9.8	±	1.5
% of carbon emitted or sequestered	96.07	±	0.41

Only a small percentage of precipitation (10%) actually contributes to total river discharge. The remainder is either lost to direct evaporation from the ground, evaporation from rainfall interception, or utilized in primary productivity. Using average total carbon concentrations being exported from the North Klondike River and the calculated water budget, primary productivity can be estimated within the North Klondike river valley. This is based on the assumption that there is no significant change in carbon export, burial, and degradation from year to year.

Compared to published vales on primary productivity within boreal forests, the calculated values are lower than published values (Gower *et al.,* 2001). The lowest reported values for primary productivity are from sub-arctic evergreen boreal forests in Alaska (25 g C/m^2 to 143 g C/m^2).

However, there are multiple methods by which scientists have estimated net primary production. Gower *et al.,* (2001) directly measured biomass to estimate primary productivity, whereas Brummer *et al.,* (2012) used calculated water use efficiencies from a mathematically modelled interpretation of meteorological data to estimate primary productivity. Directly measuring primary productivity within the North Klondike River basin is logistically difficult and goes beyond the scope of this project. Primary productivity is dependent on precipitation, and although annual precipitation is recorded within the North Klondike River valley, it is only monitored at one point. There could be an uneven distribution of precipitation on different facing slopes, as well as within the park. The estimated amount of forested land area could have been incorrectly estimated, as the amount of precipitation lost to rainfall interception would change. Furthermore, species composition changes as altitude increases (Kojima, 1996), and is difficult to estimate based on satellite imagery. This would undoubtedly warrant different rainfall interception values. Even though our calculated primary productivity within

the basin is lower than published values, few scientists have attempted to quantify the carbon budget within an arctic catchment. A more accurate measurement of water use efficiency at such high latitudes, forested land cover, and precipitation within the basin would be necessary for a more accurate prediction.

5.6 Groundwater circulation rates

Tritium activities in precipitation are dominated by seasonal mixing of north to south air masses (stratosphere to troposphere) (Tadros*et al.,* 2014). This allows tritium originally injected into the stratosphere by nuclear explosions, a return to the troposphere. This exchange occurs primarily during late winter and in spring. Water in the troposphere is rapidly transported to the oceans and replaced about every 10 days. This keeps tritium levels relatively low in the troposphere except for the seasonal increases from the spring leak of the troposphere (IAEA, 2011).

Snow fall has been known to wash tritium from the upper atmosphere (Merlivat*, et al.*, 1973), although the amount of tritium varies according to altitude. The peak in tritium activity during May coincides with spring freshet and with temperatures above zero. Precipitation during this period falls from the atmosphere as rain, which is being injected with tritium from the stratosphere. All of these factors could contribute to the peak in tritium activity seen during spring freshet. Spring freshet is a mixing event, in which snowmelt or runoff, and precipitation are rapidly delivered to the stream. The rapid increase and decrease in tritium activities show a system that quickly responds to precipitation and runoff, with relatively quickly moving groundwater. Average tritium activity within the basin is 10.8 TU, dating groundwater ages to less than 10 years (Clark and Fritz, 1997).

5.7 Hydrograph Separation and Flow Pathways

Results from the two component hydrograph separation, in conjunction with the stream hydrograph, show a groundwater dominated system. Evidence that groundwater is the principal contributor to total stream discharge during winter is suggested by no observed change in dissolved solute concentrations or ^{14}C activities between January and April.

This interpretation is supported by general agreement between the four different 2-component mixing models. The four models show different calculated contributions of runoff beginning during spring freshet and continuing into the summer. The mixing model using calcium as a

tracer shows groundwater as a more significant contributor to spring freshet than precipitation or runoff. As the 2-component hydrograph is a very simple mixing model, it is not surprising to see small differences depending on the chosen tracers.

Following spring freshet, runoff and precipitation dominates the hydrograph from spring into summer. This is can be attributed to precipitation events and irregular snowmelt cycles (Boucher, 2009). It is not until July that groundwater begins to dominate the hydrograph, shown by an increase in geogenic solutes. It is thought that warmer temperatures during the summer and infiltrating precipitation would bring heat into the ground thawing permafrost and recharging groundwater. This extra heat and thawing permafrost is expected to enhance groundwater delivery to the surface by creating deeper flow pathways (Carey *et al.*, 2012; Walvoord and Striegl, 2007; O'Donnell *et al.*, 2012).

The most commonly accepted model of permafrost suggests a strong impermeable barrier isolating surface flow from deeper flow networks. The data collected from the North Klondike River during 2014 support a groundwater dominated system that rapidly responds to melt water and precipitation. Groundwater is most commonly recharged at higher elevations. The most elevated areas of this region have little to no ice content, with ground cover primarily cobbles, boulders, and exposed rock units. However, recharge and flow into deeper aquifers and groundwater could not be exclusively through these regions as the river shows a very rapid response to melt water and precipitation. A more appropriate model of flow pathways would have to include multiple recharge zones at lower elevations.

Authors have previously dismissed the potential contribution of subsurface groundwater to total river discharge, especially during spring freshet (Caret and Woo, 2001; Carey and Quinton, 2004). However this groundwater is necessary to reconcile solute balancing within the system (Boucher and Carey, 2010). A simple conceptual model can be applied to the system, with talik or thawed permafrost beneath the river and lower valley slopes, allowing near-surface groundwater a short pathway to discharge into the river. When meltwater enters these pathways, acting as a plug flow, it would force existing groundwater through the system to exit into the river as discharge. It is unlikely that recharge pathways through fractured rocks on mountain slopes are responsible for the observed increase in winter discharge or as a significant contributor to spring freshet, as the river responds almost immediately to meltwater.

6. Conclusion

This thesis explores groundwater contribution to total river discharge, and carbon sources and budget in a sub-arctic catchment. The North Klondike River is a spring fed sub-alpine river catchment within a discontinuous permafrost environment, strongly influenced by snow melt and precipitation. This is the second study done within this basin (excluding all geological mapping), and the first to examine seasonal groundwater contribution and carbon budget in the North Klondike River valley. The 2014 hydrograph shows slight differences to that of previous years, which had a smaller snowpack and subsequently a smaller maximum discharge event.

Stable isotopes in water (oxygen-18 and deuterium) and tritium help in identifying the source of the water within the catchment. Water taken from the North Klondike River plots very closely to the LMWL established at Dawson City Airport, suggesting meteorological recharge of the North Klondike. Looking more closely at the data, a seasonal shift in values can be seen associated with enrichment of the snowpack during melting. Despite the seasonal variability between samples, discharge is highly attenuated as values cluster near the mean without the spread seen in precipitation. Tritium activities are relatively low within the river but show a large spike during spring freshet, concurrent with the seasonal injection of tritium into the lower atmosphere and the contribution of snowmelt. Tritium activity dates groundwater within the system to less than 10 years.

During the winter months, before spring freshet, the North Klondike is dominated by groundwater. The small amount of DOC being exported from the basin during the winter is old and degraded. This is supported by more enriched $\delta^{13}C$ values and older ^{14}C activities, indicative of organics undergoing biodegradation. During the winter, total river discharge remains consistent with no significant changes in dissolved solutes concentrations. Despite local warming events in the valley shrinking the snowpack, there are no changes to winter baseflow or groundwater discharge recorded in the hydrograph.

The spring freshet shows the greatest release of more modern organic carbon (0.94 pMC), before quickly dropping off to almost pre-freshet concentrations. DOC $\delta^{13}C$ values after spring freshet are more depleted, most likely coming from near surface flow pathways. This

is further supported by the increase in the K:Ca ratio. Groundwater is the greatest source of DIC within the catchment, and shows little variation throughout the hydrograph. The most significant DIC concentration changes are hypothesized to be a Black Shale creek early melting event, dilution during spring freshet, and a dilution again in June with storm events and snow melt. DIC $\delta^{13}C$ values show no significant changes, and only minor fluctuations throughout the year. ^{14}C activities of DIC remain consistent through the winter, and rise to more modern values after spring freshet. There is a short drop in $^{14}C/^{12}C$, associated with the proposed Black Shale creek melting event, representing a greater contribution of older, inorganic carbon in deep groundwater.

Dissolved solute concentrations are at their highest during the winter, associated with groundwater and deeper sub-surface flow. Spring freshet sees a dilution in solutes from snowmelt and precipitation, and the activation of near surface flow pathways and the development of the active layer, as shown by the increase in K:Ca ratios. However, the influence of these surface reservoirs is short lived, and by late summer their contribution to total river discharge is minimal.

Although discontinuous permafrost is thought to restrict the capacity for precipitation and meltwater to influence groundwater discharge, the results from this paper suggest otherwise. The river seems to respond very quickly to even the smallest of melting events with an increase in groundwater discharge. The previous model of permafrost restricting the interaction between surface and deeper flow pathways is something that will need to be revisited and revised. The importance of talik, in not only allowing groundwater to discharge at the surface, but in also allowing meltwater and precipitation to quickly enter deeper flow pathways stimulating groundwater discharge is something that needs to be researched further.

The calculated carbon budget within the basin is lower than published values for boreal forest biomes. This deviation could be a result of overly conservative estimates of forested land cover, the use of a single precipitation monitoring station, and overestimated water use efficiencies.

This research contributes to our understanding of northern hydrology and carbon cycling, and how they can be expected to change in the future. The need for such research in the Arctic is of importance in view of mounting pressure for northern resource development.

Bibliography

Aiken G, Spencer R, Striegl R, Schuster P, Raymond P. (2014). Influences of glacier melt and permafrost thaw on the age of dissolved organic carbon in the Yukon River basin. Global Biogeochemical Cycles. 525-537.

Anderson L, Abbott M, Finney B, Burns S. (2005). Regional atmospheric circulation change in the North Pacific during the Holocene inferred from lacustrine carbonate oxygen isotopes, Yukon Territory, Canada. Quaternary Research 64, 21-35.

Blasch KW, Bryson JE. (2007). Distinguishing Sources of Ground Water Recharge by Using 2H and 18O. Ground Water. Vol. 45, No. 3, 294-308.

Boucher JL, Carey SK. (2010). Exploring runoff processes using chemical, isotopic and hydrometric data in a discontinuous permafrost catchment. Hydrology Research, Vol 41.6.

Boucher, J. L. (2009). A Case Study Evaluating Runoff Generation in a Subarctic Catchment Using Stable Isotope, Hydrochemical and Hydrometric Data. Master Thesis. Carleton University, Ottawa, Ontario, Canada.

Brummer C, Black TA, Jassal RS, Gran NJ, Spittlehouse DL, Chen B, Nesic Z, Amiro BD, Arain MA, Barr AG, Bourque CPA, Coursolle C, Dunn AL, Flanagan LB, Humphreys ER, Lafleur PM, Margolis HA, McCaughey JH, Wofsy SC. (2012). How climate and vegetation type influence evaportranspiration and water use efficiency in Canadian forest, peatland, and grassland ecosystems. Agricultural and Forest Meteorology 153, 14-30.

Burn, C.R. (1998). The Active Layer: Two Contrasting Definitions. Permafrost and Periglacial Processes. 9: 411-416.

Buttle JM. (1994). Isotope hydrograph separations and rapid delivery of pre-event water from drainage basins. Progress in Physical Geography 18, 1, pp. 16-41.

Carey SK, Quinton WL. (2004). Evaluating snowmelt runoff generation in a discontinuous permafrost catchment using stable isotope, hydrochemical and hydrometric data. Nordic Hydrology. Vol 35, No 4, 309-324.

Carey, S. K., & Pomeroy, J. W. (2009, January). Progress in Canadian Snow and Frozen Ground Hydrology, 2003-2007. Canadian Water Resources Journal.

Carey, S. K., & Quinton, W. L. (2005). Evaluating runoff generation during summer using hydrometric, stable isotope and hydrochemical methods in a discontinuous permafrost alpine catchment. Hydrological Processes, 19(1), 95–114.

Carey, S. K., Boucher, J. L., Duarte, C. M. (2012). Inferring groundwater contributions and pathways to streamflow during snowmelt over multiple years in a discontinuous permafrost subarctic environment (Yukon, Canada). Hydrogeology Journal, 21(1), 67–77.

Chapin FS III, Shaver GR. (1996). Physiological and growth responses of Arctic plants to a field experiment simulating climatic change. Ecology 77: 822–840.

Church M. (1974). Hydrology and permafrost with reference in northern North America. In: Proceedings of the workshop seminar on permafrost hydrology. Canadian National Committee. IHD, Ottawa, 7-20.

Clark, I. and Fritz, P. (1997). Environmental Isotopes in Hydrogeology. Lewis Publishing, New York.

Clark, I.D., 2015. Groundwater Geochemistry and Isotopes. CRC Press, Boca Raton, Florida, 427 pp.

Conant, R.T., Ryan, M.G., Ågren, G.I., Birge, H.E., Davidson, E.A., Eliasson, P.E., Evans, S.E., Frey, S.D., Giardina, C.P., Hopkins, F.M., Hyvönen, R., Kirschbaum, M.U., Lavallee, J.M., Leifeld, J., Parton, W.J., Steinweg, J.M., Wallenstein, M.D., Wetterstedt, J.Å., Bradford, M.A. (2011). Temperature and soil organic matter decomposition rates e synthesis of current knowledge and a way forward. Global Change Biology 17.

DeWalle DR, Swistock BR, Sharpe WE. (1988). Three-component tracer model for stormflow on a small Appalachian forested catchment. Journal of Hydrology. 104 (1–4), 301–310.

Dingman, S. Lawrence. (2008). Physical Hydrology. 2nd ed. Long Grove, IL: Waveland Press Inc.

Dirmeyer, P. a., Gao, X., Zhao, M., Guo, Z., Oki, T., Hanasaki, N. (2006). GSWP-2: Multimodel Analysis and Implications for Our Perception of the Land Surface. Bulletin of the American Meteorological Society, 87(10), 1381–1397.

Elsenbeer, H., Lack, A. & Cassel, K. 1995 Chemical fingerprints of hydrological compartments and flow paths at La Cuenca, western Amazonia. Water Resource. Res. 31, 3051–3058.

Environment Canada. (2012). Historical Weather. Retrieved from: http://climate.weather.gc.ca/climateData/dailydata_e.html?timeframe=2&Prov=YT&StationID=1535&dlyRange=1976-02-01|2014-10-31&Year=1976&Month=4&Day=01

Environment Yukon. (2014). North Klondike River Valley Weather. Retrieved from: https://datagarrison.com/users/300034012127970/300234011202310/plots.php?plot=3

Flannigan MD, Logan KA, Amiro BD, Skinner WR, Stocks BJ. (2005). Future area burned in Canada. Climatic Change 72: 1–16.

Frey, K. E., & McClelland, J. W. (2009). Impacts of permafrost degradation on arctic river biogeochemistry, 182, 169–182.

Frey, K. E., Siegel, D. I., Smith, L. C. (2007). Geochemistry of west Siberian streams and their potential response to permafrost degradation. Water Resources Research, 43(3).

Geological Survey of Canada, Surveys and Mapping Branch. (1972). Geology of Dawson Yukon Territory. Map 1284A. Scale 1:250,000.

Geological Survey of Canada, Surveys and Mapping Branch. (1987). Permafrost and Ground Ice Conditions of Northwestern Canada. Map 1619A. Scale 1:1,000,000.

Geyh MA. (2000). An Overview of 14C Analysis in the Study of Groundwater. Radiocarbon, Vol 42-1: 99-114.

Gibson JJ, Edwards TWD, Birks SK, St.Amour NA, Buhay WM, McEachern P, Wolfe BB, Peters DL. (2005). Progress in isotope tracer hydrology in Canada. Hydrological Processes, 19. 303-327.

Gower ST, Krankina O, Olson RJ, Apps M, Linder S, Wang C. (2001). Net Primary Production and Carbon allocation patterns of boreal forest ecosystems. Ecological Applications, 11(5). 1395-1411.

Grelle A, Lundberg A, Lindroth A, Moren AS, Cienciala E. (1997). Evaporation components of a boreal forest: variations during the growing season. Journal of Hydrology 197, 70-87.

Hartley, I.P., Hopkins, D.W., Garnett, M.H., Sommerkorn, M.,Wookey, P.A., 2008. Soil microbial respiration in arctic soil does not acclimate to temperature. Ecology Letters 11.

Hoeg S, Uhlenbrook S, Leibundgut Ch. (2000). Hydrograph separation in a mountainous catchment – combining hydrochemical and isotopic tracers. Hydrological Processes, Vol 14, 1199-1216.

Hu, X., Pollard, W.H. 1997. The hydrologic analysis and modeling of river icing growth, North Fork Pass, Yukon Territory, Canada. Permafrost and Periglacial Processes 8, 279-294.

International Atomic Energy Agency. (2001). Environmental Isotopes in the Hydrological Cycle: Principles and Applications. Water Resources Programme, Volume 2, 209-216.

Kennedy MJ, Pevear DR, Hill RJ. (2002). Mineral Surface Control of Organic Carbon in Black Shale. Science Magazine. Vol 295.

Kennedy VC, Kendall C, Zellweger GW, Wyerman TA, Avanzino RJ. (1986). Determination of the components of stormflow using water chemistry and environmental isotopes, Mattole River basin, California. Journal of Hydrology. 84 (1–2), 107–140.

Klaus J, McDonnell JJ. (2013). Hydrograph separation using stable isotopes: Review and evaluation. Journal of Hydrology, Vol 505, 47-64.

Kojima S. (1996). Ecosystem Types of Boreal Forest in the North Klondike River Valley, Yukon Territory, Canada, and their Productivity Potentials. Environmental Monitoring and Assessment, 39: 265-281.

Maclean, R., Oswood, M. W., Iii, J. G. I., Mcdowell, W. H. (2014). The effect of permafrost on stream biogeochemistry : A case study of two streams in the Alaskan (USA) taiga. 47(3), 239–267.

McGuire AD, Hayes DJ, Kicklighter DW, Manizza M, Zhuang Q, Chen M, Follows MJ, Gurney KR, McClelland JW, Melillo JM, Peterson BJ, Prinn RG. (2010). An analysis of the carbon balance of the Arctic Basin from 1997 to 2006. TELLUS B, VOL 62, NO 5.

Meglen RR. (1992). Examining large databases: a chemometric approach using principal component analysis. Marine Chemistry, 39, 217-237.

Merlivat L, Ravoire J, Vergnaud JP, Lorius C. (1973). Tritium and Deuterium content of the snow in Groenland. Earth and Planetary Science Letters 19, 235-240.

Mohammadzadeh H, Clark ID. (2008). Degradation pathways of dissolved carbon in landfill leachate traced with compound-specific 13C analysis of DOC. Isotopes in Environmental and Health Studies. Vol 44, No 3, 267-294.

Moore RD. (1989). Tracing runoff sources with deuterium and oxygen-18 during spring melt in a headwater catchment, southern laurentians, Quebec. Journal of Hydrology, Vol 112, 135-148.

Muller, SW. (1974). Permafrost or Permanently Frozen Ground and Related Engineering Problems. Edwards, Ann Arbor, MI.

Muskett RR, Romanovsky VE. (2009). Groundwater storage changes in arctic permafrost watersheds from GRACE and in situ measurements. Environmental Research Letters, 4, 045009, 8pp.

Myneni RB, Keeling CD, Tucker CJ, Asrar G, Nemani RR. (1997). Increased plant growth in the northern high latitudes from 1981 to 1991. Nature 386: 698–702.

O'Donnell, J. a., Aiken, G. R., Walvoord, M. a., Butler, K. D. (2012). Dissolved organic matter composition of winter flow in the Yukon River basin: Implications of permafrost thaw and increased groundwater discharge. Global Biogeochemical Cycles, 26(4), n/a–n/a.

Petrone, K. C., Jones, J. B., Hinzman, L. D., Boone, R. D. (2006). Seasonal export of carbon, nitrogen, and major solutes from Alaskan catchments with discontinuous permafrost. Journal of Geophysical Research, 111(G2), G02020.

Quinton WL, Marsh P. (1999). A conceptual framework for runoff generation in a permafrost environment. HydrolProc 13:2563– 2581.

Raymond PA, McClelland JW, Holmes RM, Zhulidov AV, Mul K, Peterson BJ, Streigl RG, Aiken GR, Gurtovaya TY. (2007) Flux and age of dissolved organic carbon exported to the Arctic Ocean: A carbon isotopic study of the five largest arctic rivers. Global Biogeochemical Cycles, Vol. 21, GB4011.

Rivkina E, Friedmann E, McKay C, Gilchinsky D. (2000). Metabolic Activity of Permafrost Bacteria below the Freezing Point. Applied and Environmental Microbiology. Vol. 66, No. 8.3230-3233.

Schirrmeister L, Siegert C, Kuznetsova T, Kuzmina S, Andreev A, Kienast F, Meyer H, Bobrov A. (2002). Paleoenvironmental and paleoclimatic records from permafrost deposits in the Arctic region of Northern Siberia. Quaternary International 89: 97–118.

Schurr E, Bockheim J, Canadell J, Euskirchen E, Field C, Goryachkin S, Hagemann S, Kuhry P, Lafleur P, Lee A, Mazhitova G, Nelson F, Rinke A, Romanovsky V, Shiklomanov, N, Tarnocai C, Venevsky S, Vogel J, Zimov S. (2008). Vulnerability of Permafrost Carbon to Climate Change: Implications For The Global Carbon Cycle. BioScience Magazine. Vol. 58, No.8.

Serreze, M. C., Walsh, J. E., Osterkamp, T., Dyurgerov, M., Romanovsky, V., Oechel, W. C, Barry, R. G. (2000). Observational evidence of recent change in the northern high-latitude environment, 159–207.

Shaver G, Canadell J, Chapin I, Gurevitch J, Harte J, Henry G, Ineson P, Jonasson S, Melillo J, Pitelka L, Rustad L. (2000). Global warming and terrestrial ecosystems: A conceptual framework for analysis. BioScience 50: 871–882.

Smith, L. C., Pavelsky, T. M., MacDonald, G. M., Shiklomanov, A. I., & Lammers, R. B. (2007). Rising minimum daily flows in northern Eurasian rivers: A growing influence of groundwater in the high-latitude hydrologic cycle. Journal of Geophysical Research, 112(G4), G04S47.

Spencer RGM, Aiken GR, Wickland KP, Striegl RG, Hernes PJ. (2008). Seasonal and spatial variability in dissolved organic matter quantity and composition from the Yukon River basin, Alaska. Global Biogeochemical Cycles, Vol. 22, GB4002.

St. Jacques, J.-M., Sauchyn, D. J. (2009). Increasing winter baseflow and mean annual streamflow from possible permafrost thawing in the Northwest Territories, Canada. Geophysical Research Letters, 36(1), L01401.

St-Jean, G. (2003). Automated Quantitative and Isotopic (13C) Analysis of Dissolved Inorganic Carbon and Organic Carbon in Continuous-flow Using a Total Organic Carbon Analyser. Rapid Communication in Mass Spectrometry, 17, 418-428.

Tadros CV, Hughes CE, Crawford J, Hollins SE, Chisari R. (2014). Tritium in Australian precipitation: A 50 year record. Journal of Hydrology 513, 262-273.

Taylor S, Feng X, Williams M, McNamara J. (2002). How isotopic fractionation of snowmelt affects hydrograph separation. Hydrological Processes. Vol 16, 3683-3690.

van Everdingen, RO. (1976). Geocryological terminology. Canadian Journal of Earth Sciences. 13, 862-867.

Vitousek PM, Aber JD, Howarth RB, Likens GE, Matson PA, Schindler DW, Schlesinger WH, Tilman DG. (1997). Human Alteration of the Global Nitrogen Cycle: Sources and Consequences. Ecological Applications, 7(3), 737-750.

Walvoord, M.A., Striegl, R. G. (2007). Increased groundwater to stream discharge from permafrost thawing in the Yukon River basin: Potential impacts on lateral export of carbon and nitrogen. Geophysical Research Letters, 34(12), L12402.

Woo, M. K. (2012). Permafrost Hydrology. Springer, Heidelberg, 563.

Woo, M., Kane, D. L., Carey, S. K., Yang, D. (2008). Progress in Permafrost Hydrology in the New Millennium, 254(March), 237–254.

Yuan, W., Liu, S., Liu, H., Randerson, J. T., Yu, G., Tieszen, L. L. (2010). Impacts of precipitation seasonality and ecosystem types on evapotranspiration in the Yukon River Basin, Alaska. Water Resources Research, 46(2).

Yukon Ecoregions Working Group, 2004. Yukon Coastal Plain. In: Ecoregions of the Yukon Territory: Biophysical properties of Yukon landscapes, C.A.S. Smith, J.C. Meikle and C.F. Roots (eds.), Agriculture and Agri-Food Canada, PARC Technical Bulletin No. 04-01, Summerland, British Columbia, p. 63-72.

Zhao-ping Y, Hua OY, Xing-liang X, Lin Z, Ming-hua S, Cai-ping Z. (2010). Effects of permafrost degradation on ecosystems. Acta Ecologica Sinica 30, 33-39.

Zimov SA, Schuur EAG, Chapin FS III. (2006). Permafrost and the global carbon budget. Science 312: 1612–1613.

Appendix

Geochemical analysis of precipitation, including rain and snowmelt. Concentrations are expressed as ppm.

	Ca	K	Mg	Na	Fe	F	Cl	SO_4	NO_3
Rainwater									
16-Jun-2014	0.21	1.27	1.74E-03	0.39	0.13	3.10E-03	0.38	0.20	0.06
1-Jun-2014	1.63	1.86	1.17E-02	1.67	0.43	6.80E-03	2.61	1.46	0.28
19-Jul-2014	0.43	0.79	1.67E-03	0.57	0.09	2.50E-03	0.43	0.46	0.19
13-Jul-2014	0.67	1.80	2.73E-03	1.55	0.19	1.60E-03	1.23	0.75	0.63
8-Jul-2014	0.38	0.39	3.80E-03	0.42	0.10	3.00E-04	0.73	0.29	0.27
25-Jun-2014	0.77	0.95	1.96E-03	1.21	0.17	8.00E-04	0.81	1.18	0.14
25-Jun-2014	0.13	0.31	3.02E-03	0.40	0.02	1.70E-03	0.46	0.34	0.09
13-Jul-2014	< LOD	0.41	2.90E-03	0.28	0.02	2.74E-02	0.35	0.17	0.15
27-Jun-2014	0.33	0.96	3.39E-03	0.76	0.09	2.70E-03	2.11	0.58	0.14
26-Jun-2014	0.52	0.70	< LOD	0.64	0.09	7.02E-02	0.56	0.20	0.06
14-Aug-2014	0.26	0.54	1.81E-03	0.61	0.07	1.70E-03	1.14	0.48	0.03
28-July-2014	0.11	0.54	2.28E-03	0.34	0.02	1.88E-02	0.23	0.18	0.02
Snowmelt									
14-Nov-2014	0.24	< LOD	1.65E-03	< LOD	0.03	4.00E-04	0.22	0.14	0.00
28-Nov-2014	0.93	0.60	2.30E-03	0.15	0.12	1.50E-03	0.73	0.45	0.00

Carbon-13 analysis of North Klondike River water and sampled tributaries.

	Date	ppm C DOC	δ 13 DOC	ppm C DIC	δ 13 DIC
North Klondike	07-Jan-14	0.71	-22.14	14.06	-8.70
North Klondike	21-Jan-14	0.59	-20.89	13.81	-8.51
North Klondike	03-Feb-14	0.58	-22.37	14.65	-8.79
North Klondike	18-Feb-14	0.66	-22.71	15.20	-8.89
North Klondike	04-Mar-14	0.62	-22.13	14.63	-8.72
North Klondike	19-Mar-14	0.54	-21.09	15.91	-8.78
North Klondike	01-Apr-14	0.52	-20.53	15.11	-8.70
North Klondike	15-Apr-14	0.65	-20.49	26.68	-8.24
North Klondike	18-Apr-14	0.69	-26.98	20.59	-9.14
North Klondike	23-Apr-14	6.73	-27.06	17.5	-10.31
North Klondike	10-May-14	8.48	-27.62	12.45	-9.09
North Klondike	13-May-14	4.63	-27.06	14.67	-8.73
North Klondike	14-May-14	4.18	-26.87	14.61	-8.81
North Klondike	17-May-14	2.41	-26.53	15.29	-8.18
North Klondike	19-May-14	2.49	-26	14.94	-7.96
North Klondike	20-May-14	2.12	-24.59	16.25	-8.05
North Klondike	06-Jun-14	1.62	-27.31	8.17	-8.01
North Klondike	24-Jun-14	1.12	-26.29	8.48	-5.63
North Klondike	16-Jul-14	1.24	-25.70	10.98	-6.99

North Klondike	06-Aug-14	1.16	-25.80	12.86	-7.04
North Klondike	12-Aug-14	1.25	-26.51	16.81	-7.24
North Klondike	19-Aug-14	2.13	-26.04	16.32	-7.58
Bensen Creek	18-Apr-14	0.5	-26.7	10.0	-9.8
Bensen Creek	13-May-14	2.6	-27.4	6.2	-10.7
Bensen Creek	18-Aug-14	1.99	-26.8	4.0	-2.7
Black Shale	17-Apr-14	1.6	-25.5	36.0	-5.1
Black Shale	11-May-14	5.9	-27.5	9.4	-6.2
Black Shale	18-Aug-14	0.95	-26.0	19.7	-2.3
Scout Car	17-Apr-14	0.5	-27.5	5.8	-7.4
Scout Car	14-May-14	1.4	-26.8	3.5	-7.2
Scout Car	18-Aug-14	1.13	-26.9	2.4	3.9
Grizzly Creek	17-Apr-14	2.0	-27.5	6.7	-17.3
Grizzly Creek	14-May-14	2.9	-26.8	6.6	-8.5
Grizzly Creek	18-Aug-14	1.35	-26.6	5.4	-2.5

Deuterium and ocygen-18 analysis of North Klondike River water, sampled tributaries, and precipitation.

Sample Type	**Date**	**δ 2H**	**δ 18O**
North Klondike	07/01/2014	-171.57	-22.01
North Klondike	21/01/2014	-173.77	-22.22
North Klondike	03/02/2014	-173.97	-22.08
North Klondike	18/02/2014	-174.56	-22.03
North Klondike	04/03/2014	-173.54	-21.87
North Klondike	19/03/2014	-174.78	-22.10
North Klondike	01/04/2014	-174.64	-22.05
North Klondike	15/04/2014	-174.76	-22.04
North Klondike	18/04/2014	-172.91	-21.87
North Klondike	23/04/2014	-175.37	-22.45
North Klondike	10/05/2014	-177.66	-22.94
North Klondike	13/05/2014	-176.53	-22.08
North Klondike	14/05/2014	-181.77	-23.06
North Klondike	14/05/2014	-174.50	-22.36
North Klondike	17/05/2014	-175.43	-22.10
North Klondike	19/05/2014	-174.40	-22.27
North Klondike	20/05/2014	-174.73	-22.80
North Klondike	09/06/2014	-172.88	-22.32
North Klondike	24/06/2014	-171.08	-22.67
North Klondike	16/07/2014	-168.99	-22.30
North Klondike	06/08/2014	-169.92	-22.22
North Klondike	12/08/2014	-167.83	-21.92
North Klondike	19/08/2014	-167.93	-22.11
Bensen Creek	17/04/2014	-169.74	-20.78

Bensen Creek	13/05/2014	-173.29	-21.70
Scout Car Creek	17/04/2014	-171.11	-21.01
Scout Car Creek	14/05/2014	-172.98	-22.56
Black Shale Creek	17/04/2014	-180.62	-23.35
Black Shale Creek	14/05/2014	-179.76	-23.26
Grizzly Creek	17/04/2014	-199.36	-25.99
Grizzly Creek	14/05/2014	-145.73	-14.32
Carine Creek	17/05/2014	-130.88	-8.47
Rain Water	16/01/2014	-217.75	-27.94
Rain Water	26/06/2014	-213.20	-26.83
Rain Water	20/09/2013	-199.89	-25.99
Snow Melt	28/11/2013	-191.71	-24.81
Rain Water	28/07/2014	-193.10	-23.72
Rain Water	24/04/2014	-183.34	-23.69
Rain Water	26/06/2014	-182.00	-21.94
Rain Water	06/10/2013	-166.56	-21.60
Rain Water	21/06/2014	-176.00	-20.67
Rain Water	02/10/2013	-162.10	-20.66
Rain Water	25/06/2014	-171.60	-20.63
Rain Water	09/09/2013	-162.12	-19.80
Rain Water	17/09/2013	-152.83	-19.37
Rain Water	21/04/2013	-163.47	-19.20
Rain Water	13/07/2014	-157.20	-19.11
Rain Water	25/06/2014	-157.80	-19.04
Rain Water	23/08/2014	-156.63	-18.94
Snow Melt	14/11/2013	-143.42	-18.88
Rain Water	26/06/2014	-160.20	-18.85
Rain Water	26/09/2013	-136.52	-18.77
Rain Water	23/09/2013	-137.22	-18.40
Rain Water	01/06/2014	-147.90	-18.31
Rain Water	14/08/2014	-153.20	-17.68
Rain Water	14/10/2013	-142.77	-17.43
Rain Water	14/10/2013	-142.71	-17.42
Rain Water	20/09/2013	-135.63	-17.33
Rain Water	08/07/2014	-140.40	-16.11
Rain Water	13/07/2014	-140.30	-16.07
Rain Water	27/09/2013	-129.66	-15.84
Rain Water	11/09/2013	-126.58	-15.82
Rain Water	22/09/2013	-129.52	-15.14
Rain Water	14/06/2014	-136.30	-14.42
Rain Water	31/08/2013	-130.89	-14.10
Rain Water	19/07/2014	-119.80	-13.98
Rain Water	17/08/2013	-110.28	-13.96

Rain Water	08/09/2013	-119.89	-13.85
Rain Water	19/09/2013	-116.85	-13.82
Rain Water	02/09/2013	-117.46	-13.81
Rain Water	15/07/2014	-128.30	-13.58
Rain Water	31/08/2013	-113.01	-13.18
Rain Water	03/09/2013	-114.37	-12.66
Rain Water	01/08/2013	-106.59	-12.36
Rain Water	11/06/2014	-123.60	-11.87
Rain Water	24/08/2013	-115.55	-11.83
Rain Water	06/06/2014	-126.20	-11.33
Rain Water	31/05/2014	-114.80	-11.09
Rain Water	17/08/2013	-98.67	-9.42